Coordinated routing of electric commercial vehicles with intra-route recharging and en-route battery swapping

Ramin Raeesi*

Centre for Logistics and Heuristic Optimisation (CLHO), Kent Business School, University of Kent, Chatham ME4 4TE, UK, r.raeesi@kent.ac.uk

*(*Corresponding Author)*

Konstantinos G. Zografos

Centre for Transport and Logistics (CENTRAL), Department of Management Science, Lancaster University Management School, Lancaster LA1 4YX, UK, k.zografos@lancaster.ac.uk

Abstract

A primary challenge in goods distribution using Electric Commercial Vehicles (ECVs) pertains to tackling their limited driving range. This paper proposes a multi-faceted approach towards increasing the driving range of ECVs by coordinating the options of: (i) intra-route recharging at an intermediate Recharging Station (RS), with (ii) synchronised en-route battery swapping services performed by Battery Swapping Vans (BSVs) at a pre-planned rendezvous time and space. We introduce and solve a variant corresponding to an Electric Vehicle Routing Problem with Time Windows, RSs and Synchronised Mobile Battery Swapping (EVRPTW-RS-SMBS). In the proposed model, route planning is carried out synchronously for two interdependent fleets, i.e., ECVs and BSVs, which work in tandem to complete the delivery tasks. To address methodological complications arising from the simultaneous consideration of intra-route recharging at RSs and the synchronised battery swapping on-the-fly, the paper develops a pre-optimisation procedure based on a Non-Dominated Path Identification (NDPI) algorithm that is used in deriving a significantly strengthened path-based formulation of the problem, and an efficient dynamic programming based heuristic algorithm. To gain practical insights on the economic and environmental added value and viability of the proposed logistics model, we compare different scenarios for goods distribution using ECVs in urban and regional levels in London and Southeast England, respectively. A set of numerical experiments are further performed to demonstrate the efficiency of the proposed algorithms. Our results indicate significant cost and emissions savings and an opportunity for going beyond last mile local deliveries using ECVs with the proposed logistics model.

Keywords: Routing; electric vehicles; recharging; battery swapping; scheduling and synchronisation

1. Introduction

Road freight distribution consumes around 50% of all diesel fuel and is responsible for 80% of the global net increase in diesel use since 2000 (ITF, 2018). It makes a sizeable contribution towards CO_2 emissions and is ranked first globally for total energy consumption and emissions growth (ITF, 2018). Logistics adoption of Electric Commercial Vehicles (ECVs), which are characterised by zero local emissions, has been perceived as a primary measure towards decarbonising the road freight sector at the urban and regional levels. However, a widespread adoption of ECVs by logistics fleet is still significantly hindered by their limited driving range.

The prevailing approach to tackle the issue of 'range anxiety' in goods distribution using ECVs is to pre-plan detours in their delivery routes to visit available Recharging Stations (RSs) for refuelling (Schneider et al., 2014). Intra-route recharging at an RS, however, is associated with several practical limitations. One key limitation in this regard corresponds to the RS's ownership. In practice, due to several regulatory and operational reasons, logistics companies running on ECVs need to privately own their RSs (Worley et al. 2012, Sweda et al. 2017, Kullman et al. 2018, Montoya et al. 2017, Froger et al. 2019, Raeesi and Zografos, 2020). In particular, public RSs availability at any given time period is subject to uncertainty and any pre-planned visit to these RSs may be disrupted. Also, in most cases, ECVs are prohibited from using the public network of RSs (see for example Tesla's Supercharger Fair Use Policy). At the same time, setting up an RS can be significantly costly and companies may be able to invest on opening only a few of them. Therefore, RSs that could be visited for intra-route recharging over the course of an ECV delivery route are usually few and unevenly distributed, and a large diversion in the original route may be required. The recharging time required to refill an ECV at an RS is also large, and therefore, the makespan of the routes planned based on intra-route recharging and the total number of ECVs required could be considerably larger in comparison with solutions based on the use of conventional Internal Combustion Engine Vehicles (ICEVs). Due to these practical complications, many existing companies with ECVs in their fleet, are reluctant to intra-route recharging and mostly rely on overnight recharging at their depots and using their ECVs for short delivery routes only.

To overcome these complications, and as an alternative approach to intra-route recharging for extending the driving range of ECVs, 'synchronised mobile battery swapping' has been recently proposed by Raeesi and Zografos (2020). The authors propose the Electric Vehicle Routing Problem with Time Windows and Synchronised Mobile Battery Swapping (EVRPTW-SMBS) where route planning is carried out in two interdependent levels for the ECVs delivering customers' demands, and for the Battery Swapping Vans (BSVs) swapping the depleted battery on an ECV with a fully charged one at a pre-determined rendezvous time and space. In the EVRPTW-SMBS, each BSV can provide the battery swapping service to multiple ECVs in one route, and each ECV can extend its driving range by requesting the battery swapping service for as many times as required with no need to divert its original delivery route. Raeesi and Zografos (2020) develop a business case for the use of BSVs in supporting the delivery routes of ECVs and show this approach can yield significant cost savings in comparison with solutions based on intra-route recharging when the setup cost of RSs is considered.

Many companies running on ECVs, however, have already (or by the time that BSVs become more widely available) established a network of privately owned RSs, and a logistics design that is purely based on the use of BSVs may require a complete re-investment in acquiring a BSV fleet and an inventory of spare battery packs. More importantly, depending on the geographical distribution of customers and RSs, and the allocated time windows in a given problem instance, the use of BSVs might trade-off with intra-route recharging, and to extent their driving range, it may be beneficial for ECVs to recharge at an RS rather than requesting a battery swapping service from a BSV, and vice versa. Therefore, the synergistic effect from a seamless integration of the two approaches can be significantly contributing to tackling the issue of "range anxiety" in goods distribution using ECVs. Thus, this paper focuses on the coordinated routing of ECVs with intra-route recharging and en-route battery swapping in the Electric Vehicle Routing Problem with Time Windows, RSs and Synchronised Mobile Battery Swapping (EVRPTW-RS-SMBS). In the EVRPTW-RS-SMBS, both options of recharging at a nearby RS and requesting a battery swapping service from a BSV at a coordinated time and space are available to ECVs when they need to extend their driving range over their delivery route. The optimal solution to a given instance of the EVRPTW-RS-SMBS yields therefore a set of energy feasible ECV delivery routes combining visits to RSs and services from BSVs such that the total number of ECVs and BSVs required and the total distance travelled by them are minimised.

While the extension of the solution space in the EVRPTW-RS-SMBS yields guaranteed improvement over both the EVRPTW with RSs (EVRPTW-RS) and the EVRPTW-SMBS, combining the required spatiotemporal synchronisation between the routes of ECVs and BSVs, and the possible intermediate visits to RSs brings in significant methodological complications that can hinder its practical implementation and deployment. To overcome these complications, this paper first develops an initial mathematical

formulation for the EVRPTW-RS-SMBS and then proposes several combinatorial results for deriving a significantly strengthened path-based formulation of the problem following the application of an exact Non-Dominated Paths Identification (NDPI) algorithm in a pre-optimisation stage. The paper further uses the proposed results and the multi-graph structure in the development of an efficient heuristic algorithm for the problem.

Recognising the fact that BSVs are still in the development stage and their viability for accelerating goods distribution using ECVs may be yet not fully realised (especially during the transition period related to the acceptance of this technology), we generate realistic urban and regional case studies in London and Southeast England to compare different business scenarios for operating on ECVs and derive useful managerial insights on the economic and environmental benefits of the combined use of BSVs and visits to RSs. The case study analysis also sheds light on an attractive opportunity for going beyond last mile local deliveries using ECVs and delivery in a wider regional level.

1.1. Contributions

The contribution of this paper is multi-fold: (i) the EVRPTW-RS-SMBS is introduced and formulated as a Mixed Integer Linear Programming (MILP) model for an ECV-BSV collaborative delivery network where the use of BSVs alongside intra-route recharging of ECVs at RSs is proposed for tackling the issue of "range anxiety" in goods distribution using electric vehicles, (ii) an exact NDPI algorithm is proposed for the identification of the set of the paths that must be retained between a pair of customers or a customer and the depot a priori, and closed form expressions are developed for the pre-computation of the paths attributes, (iii) a significantly strengthened path-based formulation of the EVRPTW-RS-SMBS and its special case, i.e., the EVRPTW-RS, is developed and its performance against the existing formulations and algorithms is demonstrated, and (iv) a Dynamic Programming (DP) based heuristic solution algorithm exploiting the proposed multigraph structure is developed to tackle practically sized instances of the problem efficiently.

In the remainder of the paper, in section 2, a survey on the most pertinent literature is presented. Section 3 of the paper describes the EVRPTW-RS-SMBS formally and establishes the required notation, definitions and assumptions. Section 4 discusses the exact and the heuristic solution algorithms. To establish a practical business case for the proposed logistics model, section 5 discusses alternative business scenarios for operating on ECVs. Section 6 presents the computational results; and finally, section 7 is the discussion and concluding remarks section.

2. Previous related work

Road freight decarbonising initiatives have been increasingly incorporated into new VRP models and solution algorithms in recent years. Incorporation of an explicit objective function pertaining to the amount of fuel consumed in emissions minimising VRPs (Bektas and Laporte, 2011; Raeesi and Zografos, 2019; Androutsopoulos and Zografos, 2017), and development of VRPs with intermediate stops for routing a fleet of vehicles operating on a cleaner alternative fuel (Erdogan and Miller-Hooks, 2012; Raeesi and O'Sullivan, 2014; Salimifard and Raeesi, 2014) or electric batteries (Conrad and Figliozzi, 2011; Bruglieri et al., 2015; Schneider et al., 2014; Desaulniers et al., 2016; Hiermann et al., 2016) have been among the most prominent research directions in VRPs with environmental considerations. In particular, the use of alternative propulsion systems to the traditional diesel (or petrol) internal combustion engines, such as biofuels, liquid or compressed natural gas, hydrogen fuel cells, and electric batteries, is increasingly perceived as a major route to greening the road freight sector. These alternative fuels, however, have a significantly smaller volumetric energy compared with diesel and gasoline, and therefore, vehicles running on them have a limited driving range. An additional operational limitation particular to electric battery operated vehicles corresponds to the larger refuelling time required to refill an electric battery in comparison with the time spent at a refuelling station by other alternative fuel vehicles.

A pervasive approach in tackling the limited driving range of ECVs for freight distribution corresponds to the introduction of minimal detours in the original delivery route of an ECV to visit an RS for recharging. In the EVRPTW-RS (Schneider et al. 2014), ECVs are permitted to visit available RSs to 'fully' recharge their battery and carry out their delivery routes. The key difference between the EVRPTW-RS and its earlier counterpart, the Green-VRP (Erdogan and Miller-Hooks, 2012), lies in the consideration of time windows and capacity constraints, and a significantly larger recharging time which is assumed linearly dependent on the State of Charge (SoC) of the ECV upon its arrival at the RS. Schneider et al. (2014) formulate the EVRPTW-RS as a MILP model on an augmented graph of the customers and RSs with sufficient dummy copies of the RSs to allow several visits to the same RS. This formulation, however, is only able to handle small-sized instances of up to 10 customers, and few instances of 15 customer nodes and 5 RSs, as the graph size grows rapidly with the increasing size of the instances. To tackle practical problem instances, Schneider et al. (2014) develop an algorithm based on the hybridisation of a variable neighbourhood search with a Tabu Search heuristic.

Research succeeding to the EVRPTW-RS, on the other hand, has primarily developed in four main directions corresponding to: (i) the consideration of partial recharging strategies (Felipe et al. 2014; Desaulniers et al. 2016; Keskin and Çatay, 2016; Froger et al. 2019; Goeke, 2019), (ii) the consideration of different recharging technologies (Felipe et al. 2014; Froger et al. 2019), (iii) the incorporation of realistic assumptions for ECV's energy consumption and battery recharging functions (Goeke and Schneider, 2015; Montoya et al. 2017; Froger et al. 2019; Basso et al. 2019), and (iv) the consideration of a mixed fleet of vehicles (Goeke and Schneider, 2015; Hiermann et al. 2016). As indicated, some of these papers integrate more than one of these aspects into the proposed models and solutions. Given the extra complications added for more accurate representations of ECVs characteristics in these problem variants, in almost all the mentioned studies, heuristic solution algorithms have been used. Exception must be, however, given to the study of Desaulniers et al. (2016) where an exact branch-price-and-cut algorithm is developed for four different variants of the EVRPTW-RS that are distinguished from one another on the basis of the recharging strategy at an RS (full or partial), and the recharging frequency over a delivery route allowed (single or multiple). There is also another stream of research that focuses on location-routing models where ECVs routing and the siting of RSs or battery swapping stations is simultaneously considered (Worley et al. 2012, Yang and Sun, 2015, Schiffer and Walther, 2017, Hof et al. 2017). Newer research has also considered areas such as the two-echelon EVRPs with battery swapping stations (Jie et al. 2019), the EVRPTW with time-dependent and stochastic waiting times at RSs (Keskin et al. 2019, 2021), the EVRP with energy consumption uncertainty (Pelletier et al. 2019), the EVRPTW with time-variant electricity prices (Lin et al. 2021), the EVRP with stochastic and time-dependent travel times (Florio et al. 2020), the EVRP with stochastic demand (Hung et al. 2021), and the EVRP with machine learning for energy prediction (Basso et al. 2021). We may also refer to recent review papers of Kucukoglu et al. (2021) and Xiao et al. (2021) on different variants of the EVRPs.

Pertinent to the current study also, we may refer to studies focusing on the development of path-based formulations for EVRPs and Green-VRPs and studying the problem on a multi-graph (Koç and Karaoglan, 2016; Andelmin and Bartolini, 2017; Froger et al. 2019). These approaches mainly focus on addressing the limitation of previous formulations pertaining to the graph augmentation with dummy nodes to represent multiple visits to a recharging/refuelling station. Koç and Karaoglan (2016) argue that in the worst case, the number of dummy nodes for each RS visit can be equal to the number of customers and as the size of the enumeration tree in MIP solvers increases exponentially with the number of binary variables, formulations based on the use of dummy nodes offer a poor performance. To address this, Koç and Karaoglan (2016) propose an alternative formulation for the Green-VRP by precomputing paths with only a single intermediate visit to a refuelling station. Andelmin and Bartolini (2017) reformulate the Green-VRP on a multigraph of non-dominated 'refuel-paths'. They define a refuel-path as a simple path starting at the depot or a customer node, passing through one or several refuelling stations and ending at another customer or the depot. Constructing a multi-graph in the context of EVRPs, on the other hand, is comparatively more difficult than in the context of the Green-VRPs, mainly because the charging time is not constant and is linearly dependent on the ECVs battery charge level upon its arrival at the RS. Froger et al. (2019) develop a path-based formulation for an EVRP with nonlinear charging function, where each path comprises intermediate visits to one or multiple RSs. The authors use several results from Zündorf (2014) for the development of a label-correcting algorithm for the identification of non-dominated paths a priori. Their proposed algorithm does not account for time-windows, but can incorporate partial recharging strategies, non-linear charging functions and multiple technologies.

As an alternative to the prevalent literature that is largely focused on 'stationary' recharging or battery swapping at intermediate RSs or battery swapping stations, Raeesi and Zografos (2020) introduce the EVRPTW-SMBS based on 'non-stationary' battery swapping services. In the EVRPTW-SMBS, a fleet of BSVs works in tandem with the ECV fleet to provide battery swapping services on-the-fly. A BSV can serve multiple ECVs in one trip without any need to divert the route of the moving ECVs, and therefore, with a small number of BSVs multiple ECVs can be served. Also, since the battery swapping service is carried out in a small fraction of the time required for recharging the ECV at an RS, the overall number and travel time of ECVs is smaller and a much higher degree of flexibility in designing delivery routes is yielded. The authors develop a methodology for the exact evaluation of an EVRPTW-SMBS solution and tackling the interdependence problem (Drexl, 2012) based on a two-stage hybridisation of a Dynamic Programming and an Integer Programming (DPIP) algorithm, which is also used in an intensified large neighbourhood search algorithm to solve practical instances of the problem.

While the above-mentioned study seems to be the only paper on the use of BSVs for supporting goods distribution routes of ECVs in a logistics context, 'non-stationary battery swapping/recharging' technologies have been increasingly exploited in a relevant stream of research focusing on mobile battery swapping/recharging 'as a service' for public EV users (Shao et al. 2017, Kosmanos et al. 2018, Abdolmaleki et al. 2019, Guo et al. 2020, Zhang et al. 2020). Shao et al. (2017) study an EVs battery swapping platform based on the service provided by a BSV. They analyse the required mobile battery swapping architecture and develop a service request priority and queuing model in which priority is defined based on the SoC of the incoming EVs into the service platform. Guo et al. (2020) introduce a subscription-based Charging-as-a-Service (CaaS) platform in which service vehicles carrying

modular battery units are dispatched to provide EVs with on-demand battery delivery. Abdolmaleki et al. (2019) study a mobile battery charging service based on the concept of on-the-move wireless power transfer between EVs, and develop a formulation and a solution algorithm for the resulting problem of routing, scheduling, and matching vehicles in the proposed vehicle-to-vehicle power transfer service platform. Zhang et al. (2020) consider a reservation-based approach in a mobile charging platform where the mobile chargers themselves have restricted charge capacity. Kosmanos et al. (2018) consider the routing of EVs in a platform where buses or trucks act as mobile charging stations moving along their normal routes, and EVs in need of charging get their required charging via wireless power transmission.

The proposed EVRPTW-RS-SMBS in this paper presents significant opportunities at the exploitation of both approaches of recharging at RSs and requesting a mobile battery swapping service for extending the driving range of delivery vehicles running on an electric battery. This is, however, a very difficult problem with technical complications (i.e., simultaneous consideration of recharging at RSs and spatiotemporally synchronised mobile battery swapping) that have not been accounted for before. To address these complications, we propose a simple, yet efficient NDPI algorithm for multigraph representation of the proposed problem in a pre-optimisation stage. We demonstrate that by just putting a strengthened path-based formulation of the EVRPTW-RS-SMBS in CPLEX, it is possible to solve instances with up to 25 customers and 21 RSs that are otherwise intractable. While our proposed NDPI algorithm is chiefly tailored for the EVRPTW-RS-SMBS, it is also adapted to derive for the first time a path-based formulation of the EVRPTW-RS of Schneider et al. (2014) that can solve instances with up to 100 customers and 21 RSs that have been only possible to approach using the sophisticated branch-price-and-cut algorithm of Desaulniers et al. (2016) previously. Concerning the simpler problem of EVRP-RS (i.e., without time windows), despite the simplifying (yet non-restrictive) assumptions we adopt regarding the charging function at RSs, our proposed algorithm has a much simpler implementation compared with the overly complex label-correcting algorithm of Froger et al. (2019) and can yet reinforce the derivation of a path-based formulation to provide a tight upper bound to the EVRP-RS when more realistic assumptions such as non-linear recharging and multiple technologies are considered. To tackle practical instances of the difficult EVRPTW-RS-SMBS, on the other hand, the proposed multigraph representation is further used in the development of an efficient DP-based heuristic algorithm for the EVRPTW-RS-SMBS.

3. The EVRPTW-RS-SMBS: formal description and formulation

In this section, we first provide a formal description of the EVRPTW-RS-SMBS and discuss the notation, definitions and key assumptions adopted by the paper. Following that, the mathematical formulation of the problem is given. A full list of the notation and acronyms used in the paper is available in Appendix A for ease of reference.

1.1. Formal description

The EVRPTW-RS-SMBS can be defined on a complete directed graph $G = (V, A)$, where the vertex set $V = \{0\} \cup N \cup R$ consists of the depot $\{0\}$, customer nodes $N = \{1,2, \dots, n\}$, and RSs $R = \{n+1, n+2, \dots, n+r\}$. Each customer $i \in N$ is associated with a demand q_i, a hard time window $[e_i, l_i\ ]$ and a service time s_i. The depot working hours, which is considered as the planning horizon, is denoted by $[e_0, l_0\ ]$. The set $A = \{(i,j) | i,j \in V, i \neq j\}$ is the set of directed arcs, and each arc $(i,j) \in A$ is associated with a distance d_{ij} and a travel time t_{ij}.

There is a homogeneous fleet of ECVs and a homogenous fleet of electric BSVs that are all fully charged and based at the depot. ECVs are responsible for delivering customers' demands and BSVs are in charge of providing battery swapping services at the requested time and space by the ECVs over their routes. The tasks of ECVs and BSVs are not interchangeable and BSVs cannot take part in delivering customers' demands as their payload is allocated to delivering/picking up spare/depleted batteries. Each ECV is associated with a maximum payload Q_e, a battery capacity C_e, and an energy consumption rate per unit distance travelled r_e. Each BSV, on the other hand, can carry a maximum number of batteries Q_b, has a battery capacity C_b, and an energy consumption rate r_b.

Similar to Schneider et al. (2014) we assume that each ECV is allowed to visit RSs for recharging its battery for the difference between its present charge level and C_e, and recharging time is assumed linearly proportional to the amount of energy recharged at a recharging rate of g. Moreover, there is no restriction on the number of times an ECV can visit RSs over its delivery route. Note that while we are adopting a simplifying assumption regarding the linearity of the recharging function due to the complexity of the proposed problem and algorithms, all results discussed in the next section of the paper can be extended to the case of a non-linear recharging function. This will be further discussed duly.

ECVs can alternatively request a battery swapping service from a BSV while at a customer location. Realistically, the battery swapping service can only start once the ECV service at the customer is over, and it is not possible to swap the ECV's battery simultaneous with it providing service at the customer. The arrival time of the BSV at the swapping location must be therefore synchronised with the ECV's service finish time. However, the BSV can arrive earlier and wait till swapping starts. It is assumed

that swapping takes λ time units, and BSVs are not allowed to require a battery swap from other BSVs during their trip. An ECV, on the other hand, can ask for a battery swap for as many times as required during its trip, and there is no restriction for a BSV to serve the same ECV multiple times.

The aim of the EVRPTW-RS-SMBS is to determine an optimal composition of ECVs and BSVs in the fleet to operate routes that start and finish at the depot. ECVs must serve every customer exactly once within their pre-defined time-windows, without violating vehicles' payload and battery capacities and working day limits, such that the following two objectives are minimised lexicographically: (i) the total number of ECVs and BSVs required, and (ii) the total travelled distance of ECVs and BSVs.

Next, an initial MILP formulation is given for the EVRPTW-RS-SMBS.

1.2. Mathematical formulation

Prior to discussing the mathematical formulation of the problem, a few auxiliary sets and notation are required for ease of reference. We assume that $\{\sigma\}$ is a dummy copy of the depot $\{0\}$ and we refer to it as the final depot where all routes terminate. To allow multiple visits to each RS in the set R, a sufficiently large set R' of dummy nodes is generated. We also define: $V' = N \cup R', V_0 = \{0\} \cup N$, $V_\sigma = N \cup \{\sigma\}, V_0' = \{0\} \cup N \cup R'$, $V_\sigma' = N \cup R' \cup \{\sigma\}$, and $\mathcal{A} = \{(i,j) | i \in V_0, j \in V_\sigma, i \neq j\}$. Note that following these definitions, the vertex set V is expanded to $V = \{0\} \cup N \cup R' \cup \{\sigma\}$ and the set of directed arcs A is better written as $A = \{(i,j) | i \in V_0', j \in V_\sigma', i \neq j\}$.

The MILP formulation of the EVRPTW-RS-SMBS works with the following decision variables:

- x_{ij}: Binary decision variable indicating if arc $(i,j) \in A$ is traversed by an ECV.
- z_{ij}: Binary decision variable indicating if arc $(i,j) \in \mathcal{A}$ is traversed by a BSV.
- y_i: Decision variable denoting the time of arrival of an ECV at node $i \in V$.
- w_i: Decision variable denoting the time of arrival of a BSV at node $i \in V \backslash R'$.
- f_i: Decision variable specifying the remaining load on an ECV upon arrival at node $i \in V$.
- h_i: Decision variable specifying the number of the remaining fully-charged battery packs on the BSV upon arrival at node $i \in V \backslash R'$.
- u_i: Decision variable indicating the remaining battery charge level of an ECV on arrival at node $i \in V$.
- v_i: Decision variable indicating the remaining battery charge level of a BSV on arrival at node $i \in V \backslash R'$.

The mathematical formulation of the EVRPTW-RS-SMBS is given by (1)-(26).

$$z_1 := \sum_{j \in V_\sigma'} x_{0j} + \sum_{j \in V_\sigma} z_{0j} \tag{1}$$

$$z_2 := \sum_{(i,j) \in A} d_{ij} x_{ij} + \sum_{(i,j) \in \mathcal{A}} d_{ij} z_{ij} \tag{2}$$

$$lex \min(z_1, z_2) \tag{3}$$

Subject to:

$$\sum_{j \in V_\sigma'} x_{ij} = 1, \qquad \forall i \in N \tag{4}$$

$$\sum_{j \in V_\sigma'} x_{ij} \leq 1, \qquad \forall i \in R' \tag{5}$$

$$\sum_{j \in V_\sigma'} x_{ji} - \sum_{j \in V_\sigma} x_{ij} = 0, \qquad \forall i \in V' \tag{6}$$

$$\sum_{j \in V_0} z_{ji} - \sum_{j \in V_\sigma} z_{ij} = 0, \qquad \forall i \in V \tag{7}$$

$$y_i + (t_{ij} + s_i) x_{ij} + \lambda \sum_{\vartheta \in V_\sigma : i \neq 0} z_{i\vartheta} - (l_0 + \lambda)(1 - x_{ij}) \leq y_j, \qquad \forall i \in V_0, j \in V_\sigma', i \neq j \tag{8}$$

$$y_i + t_{ij}x_{ij} + g(C_e - u_i) - (l_0 + gC_e)(1 - x_{ij}) \leq y_j, \qquad \forall i \in R', j \in V'_\sigma, i \neq j \tag{9}$$

$$w_i \leq y_i + s_i, \qquad \forall i \in V_0 \tag{10}$$

$$y_i + (t_{ij} + s_i + \lambda)z_{ij} - l_0(1 - z_{ij}) \leq w_j, \qquad \forall i \in V_0, j \in V_\sigma, i \neq j \tag{11}$$

$$e_i \leq y_i \leq l_i, \qquad \forall i \in V \tag{12}$$

$$0 \leq f_j \leq f_i - (q_i x_{ij}) + Q_e(1 - x_{ij}), \qquad \forall i \in V'_0, j \in V'_\sigma, i \neq j \tag{13}$$

$$0 \leq f_0 \leq Q_e \tag{14}$$

$$0 \leq h_j \leq h_i - z_{ij} + Q_b(1 - z_{ij}), \qquad \forall i \in V_0, j \in V_\sigma, i \neq j \tag{15}$$

$$0 \leq h_0 \leq Q_b \tag{16}$$

$$0 \leq u_j \leq u_i - (r_e d_{ij} x_{ij}) + (C_e \sum_{\vartheta \in V_0 : j \in N} z_{\vartheta j}) + C_e(1 - x_{ij}), \qquad \forall i \in N, j \in V'_\sigma, i \neq j \tag{17}$$

$$0 \leq u_i \leq C_e, \qquad \forall i \in V \tag{18}$$

$$0 \leq u_j \leq C_e - (r_e d_{ij} x_{ij}) + (C_e \sum_{\vartheta \in V_0 : j \in N} z_{\vartheta j}), \qquad \forall i \in \{\{0\} \cup R'\}, j \in V'_\sigma, i \neq j \tag{19}$$

$$u_i \geq \sum_{j \in V'_\sigma} r_e d_{ij} x_{ij}, \qquad \forall i \in N \tag{20}$$

$$0 \leq v_j \leq v_i - (r_b d_{ij} z_{ij}) + C_b(1 - z_{ij}), \qquad \forall i \in V_0, j \in V_\sigma, i \neq j \tag{21}$$

$$0 \leq v_i \leq C_b, \qquad \forall i \in V \backslash R' \tag{22}$$

$$x_{ij} \in \{0,1\}, \qquad \forall (i,j) \in A \tag{23}$$

$$z_{ij} \in \{0,1\}, \qquad \forall (i,j) \in \mathcal{A} \tag{24}$$

$$y_i \geq 0, f_i \geq 0, u_i \geq 0\,, \qquad \forall i \in V \tag{25}$$

$$w_i \geq 0, h_i \geq 0, v_i \geq 0\,, \qquad \forall i \in V \backslash R' \tag{26}$$

Expressions (1) and (2) are the objective functions that seek to minimise the total number of ECVs and BSVs required, and the total distance travelled by them, respectively. Expression (3) denotes the lexicographic minimisation of the two objectives in (1) and (2). Constraints (4) and (5) enforce the connectivity of customer visits and visits to recharging stations, respectively. Constraints (6) and (7) together establish flow conservation by guaranteeing that at each vertex, the number of incoming arcs is equal to the number of outgoing arcs for ECVs and BSVs, respectively. Constraints (8) determine the arrival time of an ECV at each node by

accounting for the arrival time at the upstream node, its service time, and its potentially required time for a requested swap by a BSV. Constraints (9) do so when the upstream node is an RS and account for the required recharging time to fill the battery capacity. Constraints (10) and (11) together are synchronisation constraints and ensure that a planned swap service by a BSV takes place after service at the customer is completed by the ECV. Constraints (12) enforce that every vertex is visited within its time window. Constraints (13) and (14) ensure demand fulfilment while guaranteeing that the capacity of the ECVs is not violated, and constraints (15) and (16) do the same for BSVs. Constraints (17) to (20) determine the battery charge level of ECVs after visiting a customer and/or an RS. Constraints (21) and (22) determine the battery charge of BSVs at each node and ensure the energy feasibility of BSV routes. Finally, constraints (23)-(26) define the domains of the decision variables.

It is worth mentioning that the EVRPTW-RS and the EVRPTW-SMBS are special cases of the EVRPTW-RS-SMBS. If we add constraints $\sum_{(i,j)\in\mathcal{A}} z_{ij} = 0$ to the formulation given in (1)- (26), the problem is reduced to EVRPTW-RS, and if we change constraints (5) to $\sum_{j\in V'_\sigma} x_{ij} = 0: \forall i \in R'$, the problem is reduced to EVRPTW-SMBS.

In the next section, we discuss several combinatorial results that make the development of a much more compact and strengthened path-based formulation for the EVRPTW-RS-SMBS possible. These results are also quite useful in the development of the heuristic solution algorithm for the problem.

4. An exact and a heuristic solution algorithm for the problem

The EVRPTW-RS-SMBS includes the EVRPTW-RS and the EVRPTW-SMBS and is hence a very difficult problem to tackle. Integration of the options of intra-route recharging of ECVs and the spatiotemporal coordination between ECVs and BSVs for mobile battery swapping adds extra complexity to the problem formulation and solution process. In this section we propose a significantly strengthened path-based formulation and a heuristic algorithm for the problem.

4.1. The NDPI algorithm

The initial formulation of the EVRPTW-RS-SMBS presented in section 3 relies on sufficient replications of each RS (n replications in the worst case) and can only handle small instances with very few RSs. As discussed in section 2, due to this limitation, several Green-VRP and EVRP studies (Koç and Karaoglan, 2016; Andelmin and Bartolini, 2017; Froger et al. 2019) have favoured path-based formulations to eliminate RSs from consideration. The performance of these formulations, on the other hand, relies greatly on the efficiency of the pre-processing algorithm that is used for the identification of non-dominated paths between customers and customers and the depot. In the context of the EVRPTW-RS-SMBS, the identification of non-dominated paths a priori must be carried out in the presence of customers' time windows and the option of mobile battery swapping. This is a particularly complicated task that has not been previously investigated. In this section, we discuss several combinatorial results for the development of a simple and fast algorithm for this purpose.

Given that there exists r RSs in R, there are $\sum_{i=1}^{r} \varpi_i$ (where $\varpi_i = \varpi_{i-1}(r-i+1)$, and $\varpi_0 = 1$) distinct paths between a given origin and destination node in G that pass through at least one RS. That means for a value of r as small as 6, there are 1,956 different paths between a pair of nodes in G; this increases exponentially, e.g. when $r = 10$, the number of paths increases to 9,864,100 paths. Therefore, full enumeration of paths for constructing a multigraph and deriving a path-based formulation is intractable. However, it is possible to identify many of the paths that cannot be part of an optimal solution to the EVRPTW-RS-SMBS and eliminate them from consideration. Prior to presenting several results for doing so, some terms that are used in the rest of this section are established below:

- *Required nodes:* required nodes (V_r) are the nodes on G that represent the location of the depot and the customers; i.e., $V_r = \{0\} \cup N \cup \{\sigma\}$.
- *Direct edge:* a direct edge ϵ_{ij}, or simply an edge, is hereafter an arc $(i,j) \in A | i,j \in V_r, i \neq j$.
- *RS-path:* an RS-path p_{ij}, is a sequence of arcs in A that passes through at least one RS on R and connects a pair of required nodes $i,j \in V_r, i \neq j$; i.e., $p_{ij} = [(i,1),(1,2),\dots,(n,j)], 1..n \in R$. By convention, let us assume that $\mathcal{P}_{ij}$ is the set of all possible RS-paths between a pair of required nodes, i.e., $\mathcal{P}_{ij} = \{p_{ij,1}, p_{ij,2}, \dots, p_{ij,\ell}\}$ (remember that identifying this set can be intractable).
- *Battery Charge Level (BCL):* The BCL indicates the remaining battery charge level of an ECV when departing from node $i \in V_r$ and is denoted by u_i.
- *Path attributes:* to each RS-path $p_{ij,\mathcal{J}} \in \mathcal{P}_{ij}$, several attributes such as distance and travel time could be attributed, that we henceforth call path attributes.

Most of the arguments and results presented in the following rely on the BCL at the origin node of a pair of required nodes i and j, and hence a notion called *'BCL-dependency'* is introduced below:

Definition 1 ***BCL-dependent and BCL-independent path attributes:*** *a given path attribute of an RS-path $p_{ij,\mathcal{J}} \in \mathcal{p}_{ij}$ is called a "BCL-dependent path attribute" if for its computation a knowledge of u_i is required, and its value depends on the value of u_i; on the contrary, if the value of the path attribute is unaffected by u_i it is called a "BCL-independent path attribute".*

We use a small example, shown in Figure 1, to illustrate better this notion of the BCL-dependency and the forthcoming arguments of this section. Assume the number on each arc in this figure represents both the distance and the travel time of each arc. Also, suppose $C_e = 10, r_e = 1$, and $g = 2$. Then, considering the RS-path (i, k, j) (which we call $p_{ij,1}$), it is clear that, while its distance $d(p_{ij,1})$ is BCL-independent, and regardless of the BCL at node i, is 10, its travel time $\tau^{u_i}(p_{ij,1})$ is BCL-dependent and is determined based on the value of u_i. For example, for $u_i = 7$, we have $\tau^7(p_{ij,1}) = 22$, while for $u_i = 4$, we have $\tau^4(p_{ij,1}) = 28$.

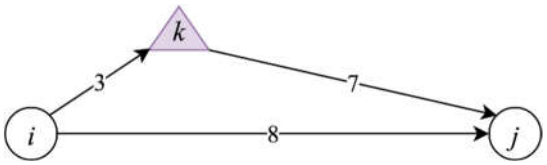

Figure 1 A small example of two required nodes and one intermediate RS

Observation 1 *Regardless of the number of RSs visited on the RS-path $p_{ij,\mathcal{J}} \in \mathcal{p}_{ij}$, knowing u_i is necessary and sufficient to compute $\tau^{u_i}(p_{ij,\mathcal{J}})$ using the closed form expression $\tau^{u_i}(p_{ij,\mathcal{J}}) = \mathbb{t}_{ij,\mathcal{J}} + g(C_e - u_i)$, where $\mathbb{t}_{ij,\mathcal{J}}$ is the travel time of $p_{ij,\mathcal{J}}$ when $u_i = C_e$.*

To demonstrate the application of the closed form expression presented in Observation 1, we refer back to the example in Figure 1. In this example, $\mathbb{t}_{ij,1} = 16$ (made up of the travel time of the arcs, i.e., 10, plus recharging time at the RS, i.e., 6), and hence for $u_i = 7$, we have $\tau^7(p_{ij,1}) = 16 + 2(10 - 7) = 22$.

We may remind that to avoid extra complexity we are assuming a linear charging function in this paper, but as discussed earlier, it is possible to extend the results in this section to the more realistic case of a non-linear charging function. For illustration only, we discuss the extension of Observation 1 (which is key to other results in this section) to the case of a non-linear recharging function in Appendix B; all other arguments could be similarly extended.

In finding non-dominated RS-paths, there is also a need to monitor the remaining charge level at the endpoint of a given RS-path. Intuitively, the higher is the endpoint BCL, the more favourable the path is, as it leaves further flexibility in travelling from the endpoint of the path to subsequent nodes along the ECV route. Since the ECV is fully charged at the last RS over a given RS-path, the endpoint BCL of any RS-path is simply equal to $C_e - \pi(p_{ij,\mathcal{J}})$, where $\pi(p_{ij,\mathcal{J}}) = r_e d_{nj}$ is the charge used at the last arc of the path, i.e., arc (n, j). In order to conform with other path attributes later used in establishing the dominance rule, however, instead of monitoring the endpoint BCL, we keep track of $\pi(p_{ij,\mathcal{J}})$ in our algorithm, and as it is the inverse of the endpoint battery charge level of the RS-path, we refer to it as the Endpoint Battery Discharge Level (EBDL) attribute of the RS-path $p_{ij,\mathcal{J}}$. It can be observed that in the case of the example in Figure 1, we have $\pi(p_{ij,1}) = 7$.

Definition 2 ***Minimum Required BCL (MR-BCL):*** *MR-BCL is a BCL-independent path attribute for a given RS-path $p_{ij,\mathcal{J}} \in \mathcal{p}_{ij}$, i.e., $\varphi(p_{ij,\mathcal{J}})$, that denotes the minimum value of u_i, below which it is not possible to start the RS-path $p_{ij,\mathcal{J}}$. Hence, $\varphi(p_{ij,\mathcal{J}}) = r_e d_{i1}$, where d_{i1} denotes the distance of the first arc in $p_{ij,\mathcal{J}}$.*

Obviously, in the case of the example in Figure 1, we have $\varphi(p_{ij,1}) = 3$.

Lemma 1 *Given two different RS-paths $p_{ij,1}, p_{ij,2} \in \mathcal{p}_{ij}$, if $\tau^{C_e}(p_{ij,1}) \leq \tau^{C_e}(p_{ij,2})$, then $\tau^{u_i}(p_{ij,1}) \leq \tau^{u_i}(p_{ij,2}), \forall u_i \in [\varphi(p_{ij,1}), C_e]$.*

Proof. See Appendix C.1.

Lemma 1 presents a useful result in the development of the intended NDPI algorithm as it implies that the comparison between the travel time of different RS-paths would be sufficient at only one BCL, i.e., the fully charged battery level. Note, however, that

this lemma does not cover values of $u_i < \varphi(p_{ij,1})$, as for such values path $p_{ij,1}$ could not be traversed. As a result, if $\varphi(p_{ij,2}) < \varphi(p_{ij,1})$, there are some u_i for which path $p_{ij,2}$ is preferred over path $p_{ij,1}$ as regards the travel time attribute.

Definition 3 ***Eligibility vector:*** *To every RS-path $p_{ij,\mathcal{J}} \in \mathcal{p}_{ij}$ a 4-dimensional (4D) vector of attributes, corresponding to $E(p_{ij,\mathcal{J}}) := [d(p_{ij,\mathcal{J}}), \tau^{Ce}(p_{ij,\mathcal{J}}), \pi(p_{ij,\mathcal{J}}), \varphi(p_{ij,\mathcal{J}})]$, is associated that is called its eligibility vector.*

Definition 4 ***Eligibility vector dominance:*** *The eligibility vector $E(p_{ij,1})$ of an RS-path $p_{ij,1} \in \mathcal{p}_{ij}$ is said to dominate another eligibility vectors $E(p_{ij,2})$ of an RS-path $p_{ij,2} \in \mathcal{p}_{ij}$ (denoted by $E(p_{ij,1}) \preccurlyeq E(p_{ij,2})$) iff $d(p_{ij,1}) \leq d(p_{ij,2}), \tau^{Ce}(p_{ij,1}) \leq \tau^{Ce}(p_{ij,2}), \pi(p_{ij,1}) \leq \pi(p_{ij,2})$ and $\varphi(p_{ij,1}) \leq \varphi(p_{ij,2})$. Consequently, if $E(p_{ij,1})$ is not dominated by the eligibility vector of any other RS-path in $\mathcal{p}_{ij}$, its eligibility vector is said to be non-dominated.*

Definition 5 ***An Eligible Path:*** *An RS-path $p_{ij,\mathcal{J}} \in \mathcal{p}_{ij}$ with a non-dominated eligibility vector $E(p_{ij,\mathcal{J}})$ is called an eligible path, and any other RS-path connecting required nodes $i, j \in V_r$ with dominated eligibility vector is called a redundant path. We denote the set of all eligible paths between a pair of required nodes $i, j \in V_r$ by $\mathfrak{p}_{ij}$.*

Theorem 1 *Suppose $\mathcal{G} = (V_r, \mathcal{P})$, with $\mathcal{P} = \bigcup_{i,j \in V_r} \mathcal{P}_{ij}$, and $\mathcal{P}_{ij} = \{\mathfrak{p}_{ij} \cup \epsilon_{ij} | i, j \in V_r\}$, is a multigraph constructed from required nodes only and the direct edges and eligible paths between them. Then, any optimal solution found for an instance of the EVRPTW-RS-SMBS on G, could be found on $\mathcal{G}$.*

Proof. See Appendix C.2.

Theorem 1 suggests that we can identify all non-dominated paths between required nodes a priori in a pre-processing stage and solve the problem on a reduced multigraph. The identification of these paths could be done rather quickly as it must be done on a very small graph of only two customers and RSs; however, before introducing an algorithm for doing so, we exploit a property, that is observed in all existing VRPTW and EVRPTW-RS benchmark test instances, to speed up the procedure by reducing the 4D eligibility vector $E(p_{ij,\mathcal{J}}) := [d(p_{ij,\mathcal{J}}), \tau^{Ce}(p_{ij,\mathcal{J}}), \pi(p_{ij,\mathcal{J}}), \varphi(p_{ij,\mathcal{J}})]$ to a 3D eligibility vector $\mathcal{E}(p_{ij,\mathcal{J}}) := [\tau^{Ce}(p_{ij,\mathcal{J}}), \pi(p_{ij,\mathcal{J}}), \varphi(p_{ij,\mathcal{J}})]$. This property corresponds to the linear dependency between travel time and distance for all arcs $(i,j) \in A$ in the form $t_{ij} = d_{ij}/\bar{v}$, where $\bar{v}$ could be viewed as the average speed in the network (in Solomon benchmark problems (1987), test instances developed by Schneider et al. (2014) and also used in Desaulniers et al. (2016), and test instances considered in this paper, $\bar{v} = 1$). An important implication of this dependency assumption that we use is that $d_{ij} \leq d_{k\ell} \Leftrightarrow t_{ij} \leq t_{k\ell}, \forall (i,j), (k,\ell) \in A$. Hence, the following Lemma allows us to use $\mathcal{E}(p_{ij})$ instead of $E(p_{ij})$ as the eligibility vector:

Lemma 2 *If $\mathcal{E}(p_{ij,1}) \preccurlyeq \mathcal{E}(p_{ij,2})$ for two RS-paths $p_{ij,1}, p_{ij,2} \in \mathcal{p}_{ij}$, then $E(p_{ij,1}) \preccurlyeq E(p_{ij,2})$.*

Proof. See Appendix C.3.

Based on these results we are ready to propose an implementation for the algorithm which must in practice search for tri-objective shortest paths between a pair of required nodes on a very small auxiliary graph of the given origin and destination and RSs only. However, using an intuitive rule it is still possible to speed up the implementation further by searching for bi-criterion shortest paths instead. In fact, we have extensively observed in our experiments that almost always when we only look for RS-paths with non-dominated $[\tau^{Ce}(p_{ij}), \pi(p_{ij})]$, the RS-path with minimum $\varphi(p_{ij})$ already exists in the returned set, and this means we do not need to carry out any further search, as it is provable that any other path will have a dominated eligibility vector. In case this is not satisfied, it is very simple to find the 'next' RS-path with minimum $\varphi(p_{ij})$ iteratively until we see it in the set.

Hence, the implementation is given in Algorithm 1. This algorithm finds the set of non-dominated paths between a pair of required nodes $o, d \in V_r$ using a modified extension of the label setting algorithm proposed by Martins (1984) for the multi-criteria shortest path problem (we modify and use the implementation proposed by Ehrgott, 2005). In this algorithm $G' = (V', A')$ is an auxiliary graph where $V' = \{\{o, d\} \cup R\}$, and $A' = \{(i,j) | i,j \in V', i \neq j\}$. A label L of a node $i \in V'$ is denoted using a tuple $L = [\tau_i, \pi_i, u_i, J, \ell_J, k]$, where τ_i stores the travel time attribute of the path represented by the label up to node i, π_i is its EBDL attribute, u_i is the BCL at node i, J represents the node from which the label was obtained, ℓ_J indicates the identifier of the label in the list of labels at node J from which L was obtained, and k is the identifier of the current label in the list of labels at node i. Note that domination rules used in lines 13 and 14 of the algorithm, are based on the first two components of the label, i.e., τ_i and π_i. The

last while loop of the algorithm (lines 20 to 23) is only executed if the path with minimum MR-BCL does not exist already in $\mathfrak{p}_{od}$. It is worth mentioning that any shortest path algorithm could be used in line 21 for the identification of the minimum MR-BCL path.

Algorithm 1 The NDPI algorithm

1 **Input** G', origin node $o \in V'$, desination node $d \in V'$, $[e_o, l_o], s_o, [e_d, l_d]\ d_{ij}, t_{ij}, \forall (i,j) \in A', C_e, r_e, g$
2 Initialise $\mathfrak{p}_{od} = \{\}$, $\mathcal{TL} = \{\}$, and $\mathcal{PL} = \{\}$.
3 Create label $L_o = [e_o, 0, C_e, 0,0,1]$ at node o and let $\mathcal{TL} := \{L_o\}$.
4 **while** $\mathcal{TL} \neq \emptyset$ **do**
5 Let label $L_i = [\tau_i, \pi_i, u_i, \not{\jmath}, \ell_{\not{\jmath}}, \not{k}]$ of node i be the lexicographically smallest label in $\mathcal{TL}$.
6 Remove L_i from $\mathcal{TL}$ and add it to $\mathcal{PL}$.
7 **for** all $j \in V'$ such that $(i,j) \in A'$ **do**
8 **if** $i = o$ **then** $\tau_j = \tau_i + t_{ij}$ **else** $\tau_j = \tau_i + g(C_e - u_i) + t_{ij}$ **end if**
9 **if** $j = d$ **then** $\pi_j = \pi_i + r_e d_{ij}$ **else** $\pi_j = 0$ **end if**
10 $u_j = C_e - r_e d_{ij}$
11 **if** $e_o + s_o + \tau_j \leq l_d$ **and** $\pi_j \leq C_e$ **then**
12 Create label $L' = [\tau_j, \pi_j, u_j, i, \ell_i, t]$ as the next label (tth label) at node j and add it to $\mathcal{TL}$.
13 Delete all temporary labels of node j dominated by L'.
14 Delete L' if it is dominated by another label of node j.
15 **end if**
16 **end for**
17 **end while**
18 Use the predecessor labels in $\mathcal{PL}$ to recover all efficient paths and add them to $\mathfrak{p}_{od}$.
19 $\vec{a} \leftarrow$ the shortest outgoing arc from o
20 **while** $\vec{a}$ is not the first arc in any of the paths in $\mathfrak{p}_{od}$ **do**
21 Find the RS-path p_{od} with minimum $\varphi(p_{od})$ and add it to $\mathfrak{p}_{od}$
22 Remove $\vec{a}$ from G'
23 $\vec{a} \leftarrow$ the shortest outgoing arc from o
23 **end while**
24 **return** $\mathfrak{p}_{od}$

In the next sub-section, we show how these results could be used in the development of a strengthened path-based formulation of the EVRPTW-RS-SMBS.

Note that all the results presented in this section could be simply generalised to the case of the EVRPTW-RS and Green-VRP, as these are special cases of the EVRPTW-RS-SMBS. We will show in the computational results section of the paper that EVRPTW-RS instances with up to 100 customers and 21 RSs could be solved to optimality using these results by just putting a path-based formulation of the problem into CPLEX.

4.2. The strengthened path-based formulation for the EVRPTW-RS-SMBS

The alternative path-based formulation is defined on the multi-graph $\mathcal{G} = (V_r, \mathcal{P})$ (refer to Theorem 1). We superimpose ϵ_{ij} over the eligible paths in $\mathcal{P}_{ij}, \forall i,j \in V_r$, and refer to each member of the set $\mathcal{P}_{ij}$ by (i,j,p), where $p \in \{1,..,|\mathcal{P}_{ij}|\}$. Hence, $(i,j,1)$ is always the direct edge (i,j) in G. As a generalisation of the closed form expression for the BCL-dependent travel time attribute, we can use the expression of the form $\alpha_{ijp} u_i + \beta_{ijp}$ for each $(i,j,p) \in \mathcal{P}_{ij}$, where parameters α_{ijp} and β_{ijp} are parameters that could be computed as follows and used as model input:

$$\alpha_{ijp} = \begin{cases} 0, & p = 1 \\ -g, & otherwise \end{cases} \tag{27}$$

$$\beta_{ijp} = \begin{cases} t_{ij}, & p = 1 \\ \mathbb{t} + gC_e, & otherwise \end{cases} \tag{28}$$

We also define here another BCL-dependent attribute for each path, called the Charge Gained and Gone (CGG) attribute. CGG takes into account the BCL at the origin of the path and any refuelling over the path, and in practice denotes the difference between the BCL at the origin node and the BCL upon the arrival at the destination using an expression of the form $\gamma_{ijp} u_i + \delta_{ijp}$ for each $(i,j,p) \in \mathcal{P}_{ij}$, where parameters γ_{ijp} and δ_{ijp} are parameters that could be pre-computed as follows and used as model input:

$$\gamma_{ijp} = \begin{cases} 0, & p = 1 \\ 1, & otherwise \end{cases} \quad (29)$$

$$\delta_{ijp} = \begin{cases} r_e d_{ij}, & p = 1 \\ r_e d_{\ell j} - C_e, & otherwise \end{cases} \quad (30)$$

Note that CGG is not essentially non-negative.

Recycling some of the notation used in section 3 of the paper, we redefine two of the previous decision variables to use in the path-based formulation as follows:

- x_{ijp}: Binary decision variable indicating if path $(i, j, p) \in \mathcal{P}$, is traversed by an ECV.
- z_{ij1}: Binary decision variable indicating if path $(i, j, 1) \in \mathcal{P}$ is traversed by a BSV.

The alternative path-based formulation using these variables is given in Appendix D.

4.3. The heuristic algorithm

The EVRPTW-RS-SMBS is a difficult optimisation problem to tackle and the development of an efficient heuristic algorithm for the problem is a significant challenge. In the context of the EVRPTW-RS-SMBS, routing and scheduling must be carried out in two interdependent and synchronised levels for the ECVs and the BSVs in parallel, while potential intermediate visits of the ECVs to available RSs is simultaneously considered. In particular, the recursively arising problem of the 'Solution Cost Evaluation (SCE)' during the local search is per se a complicated optimisation task in the context of the EVRPTW-RS-SMBS that has not been previously encountered and addressed in other variants of the VRP. In what follows, we exploit the NDPI-based multi-graph representation discussed in the previous section in a pre-optimisation stage, and propose a dedicated Multi-Graph based DP (MG-DP) algorithm that is responsible for handling the intricate SCE problem in the EVRPTW-RS-SMBS. We then propose an efficient algorithm for tackling the EVRPTW-RS-SMBS by replacing the core DP in the DP-based Intensified Large Neighbourhood Search (DP-ILNS) algorithm of Raeesi and Zografos (2020) with the proposed MG-DP; hence calling the proposed algorithm the MG-DP-ILNS.

A 'solution' $\mathcal{S} = \{\mathcal{R}_1, \mathcal{R}_2, \dots., \mathcal{R}_k\}$ in the course of the proposed MG-DP-ILNS corresponds to a set of k capacity feasible ECV routes $\mathcal{R}_{\mathscr{k}}, \forall \mathscr{k} \in \{1, .., k\}$ that collectively visit all customers in N exactly once. Each route $\mathcal{R}_{\mathscr{k}} = \{c_0, c_1, \dots, c_\ell, c_\sigma\}$, on the other hand, is a sequence of customer visits for a given ECV that starts at the depot $\{c_0\}$, visits a set of customers $\{c_1, \dots, c_\ell\}$ and terminates at the final depot $\{c_\sigma\}$. Therefore, a solution only contains information about a set of ECV routes denoting the sequence of customer visits and does not imply any other information regarding the visits to available RSs and the time and locations of requested battery swapping services. Thereby, SCE in the context of EVRPTW-RS-SMBS entails determining the schedules for the required visits to available RSs and the calls to the battery swapping service, and thus the routes of the BSVs. On a multi-graph $\mathcal{G}$, SCE for a newly generated EVRPTW-RS-SMBS solution in the course of the MG-DP-ILNS is reduced to solving a set of Fixed Sequence Arc Selection Problems (FSASPs) (Garaix et al., 2010) that are followed by a label-selection problem optimisation as proposed in Raeesi and Zografos (2020). To Solve the emerging FSASPs, on the other hand, an extension of the DP proposed by Garaix et al. (2010) can be used. With this approach we can efficiently handle potential visits to RSs by representing non-dominated RS-paths as potential arcs between the required nodes with specific distance, travel time and fuel consumption attributes. Alongside solving the emerging FSASP, our proposed MG-DP is designed to explore the possibility of battery swaps when extending the labels along an ECV route.

The detail of the MG-DP for SCE within the EVRPTW-RS-SMBS is presented in Algorithm 2. This algorithm takes the multigraph $\mathcal{G}$, an ECV route $\mathcal{R} = \{c_0, c_1, \dots, c_\sigma\}$ (where c_0 and c_σ are the depot), and the time-windows and service times of the customers on the route in its input (line 1), and returns a set of non-dominated labels $\mathcal{L}_\sigma$ (containing the optimal evaluation) at the destination node of the given route (i.e., at the final depot). Along with $\mathcal{L}_\sigma$, and associated with each label in $\mathcal{L}_\sigma$, the algorithm returns also information about the customers that require a swapping service in $\mathcal{C}_\sigma$, and the time at which these customers need the service to be available in $\mathcal{T}_\sigma$ (line 34). To this end, the algorithm retains and extends a set of labels $\mathcal{L}_i, \mathcal{C}_i$, and $\mathcal{T}_i$ at each node c_i along $\mathcal{R}$. Each label $\ell \in \mathcal{L}_i$ is a tuple of length 3, where ℓ_1 stores the accumulated distance, ℓ_2 stores the accumulated travel time, and ℓ_3 stores the available BCL up to the current node in $\mathcal{R}$. Each monitoring label $\mathscr{g} \in \mathcal{C}_i$ and $\mathscr{f} \in \mathcal{T}_i$, on the other hand, is an open-ended list of customers requiring swaps and their requested service time, respectively. The first set of labels at c_0 is initiated in line 2 of the algorithm and it is extended in lines 3 to 32. In lines 25 to 30 the restriction on the available BCL is lifted and it is assumed that the ECV is ready to depart the node using a fully charged battery as a result of a potential battery swapping service by a BSV.

Algorithm 2 The MG-DP used as the SCE routine in the proposed MG-DP-ILNS

1 **Input** $\mathcal{G}, \mathcal{R}, C_e, r_e$, and $e_{c_i}, l_{c_i}, s_{c_i} \forall c_i \in \mathcal{R}$

2 Initialise $\mathcal{L}_0 = \{0,0,C_e\} = \{\}, \mathcal{T}_0 = \{\}$, and $\mathcal{C}_0 = \{\}$;

3 **for** $q = 0$ **to** $\sigma - 1$ **do**
4 **foreach:** label $\ell \in \mathcal{L}_q$ **do**
5 **for** $p = 1$ **to** $|\mathcal{P}_{c_q c_{q+1}}|$ **do**
6 **if** $\ell_3 \geq \varphi(\mathcal{P}_{c_q c_{q+1},p})$ **then**
7 $\mathbb{b} = max\{\ell_2 + s_{c_q} + \alpha_{c_q c_{q+1},p}\ell_3 + \beta_{c_q c_{q+1},p}, e_{c_{q+1}}\}$;
8 $\mathbb{c} = \ell_3 - \gamma_{c_q c_{q+1},p}\ell_3 - \delta_{c_q c_{q+1},p}$
9 **if** $\mathbb{b} \leq l_{c_{q+1}}$ **and** $\mathbb{c} \geq 0$ **then**
10 dominated := false; $\mathbb{a} = \ell_1 + d_{c_q c_{q+1},p}$;
11 $\mathcal{f}' = \mathcal{f}$; $\mathcal{g}' = \mathcal{g}$; // $\mathcal{f}$ and $\mathcal{g}$ are the ℓth lablels in $\mathcal{T}_q$ and $\mathcal{C}_q$, respectively
12 $\ell' = \{\mathbb{a}, \mathbb{b}, \mathbb{c}\}$;
13 **foreach:** label $\ell'' \in \mathcal{L}_{q+1}$ **do**
14 **if** $\ell'_1 \leq \ell''_1, \ell'_2 \leq \ell''_2, \ell'_3 \geq \ell''_3$ **and** $\mathcal{g}' \subseteq \mathcal{g}''$ **then** //if $q = \sigma - 1$: $\ell'_2 \leq \ell''_2$ and $\ell'_3 \geq \ell''_3$ are redundent
15 $\mathcal{L}_{q+1} := \mathcal{L}_{q+1} \backslash \{\ell''\}$; $\mathcal{T}_{q+1} := \mathcal{T}_{q+1} \backslash \{\mathcal{f}''\}$; $\mathcal{C}_{q+1} := \mathcal{C}_{q+1} \backslash \{\mathcal{g}''\}$;
16 **elseif** $\ell''_1 \leq \ell'_1, \ell''_2 \leq \ell'_2, \ell''_3 \geq \ell'_3$ **and** $\mathcal{g}'' \subseteq \mathcal{g}'$ **then** //if $q = \sigma - 1$: $\ell'_2 \leq \ell''_2$ and $\ell'_3 \geq \ell''_3$ are redundent
17 dominated := true; **break**;
18 **end if**
19 **end for**
20 **if** dominated = false **then**
21 $\mathcal{L}_{q+1} := \mathcal{L}_{q+1} \cup \{\ell'\}$; $\mathcal{T}_{q+1} := \mathcal{T}_{q+1} \cup \{\mathcal{f}'\}$; $\mathcal{C}_{q+1} := \mathcal{C}_{q+1} \cup \{\mathcal{g}'\}$;
22 **end if**
23 **end if**
24 **end if**
25 **if** $q \neq 0$ **and** $C_e \geq \varphi(\mathcal{P}_{c_q c_{q+1},p})$ **then**
26 **Repeat** lines 7 to 22 with following modifications:
27 In line 7: $\mathbb{b} = max\{\ell_2 + s_{c_q} + \lambda + \alpha_{c_q c_{q+1},p} C_e + \beta_{c_q c_{q+1},p}, e_{c_{q+1}}\}$;
28 In line 10: $\mathbb{c} = C_e - \gamma_{c_q c_{q+1},p} C_e - \delta_{c_q c_{q+1},p}$;
29 In line 11: , $\mathcal{f}' = \mathcal{f} \cup \{\ell_2 + s_{c_q}\}, \mathcal{g}' = \mathcal{g} \cup \{c_q\}$;
30 **end if**
31 **end for**
32 **end for**
33 **end for**
34 **return** $\mathcal{L}_\sigma, \mathcal{T}_\sigma$, and $\mathcal{C}_\sigma$.

The working of the proposed MG-DP in evaluating route [0,2,1,0] in the context of instance R104-5 form the 'computational results' section is illustrated in Figure 2. This figure shows that Algorithm 1 has identified one eligible RS-path only between each pair of consecutive visits, and hence Algorithm 2 has been run over the corresponding multigraph of these RS-paths and the direct edges. The figure illustrates the extension of the labels along the given ECV route, and shows that at the final node, we must choose between 2 non-dominated labels only; one of these labels does not rely on battery swapping services and only incorporates visits to RSs, whereas the other label involves battery swapping services at the locations of both customers 2, and 1, at times 25.23 and 63.07, respectively.

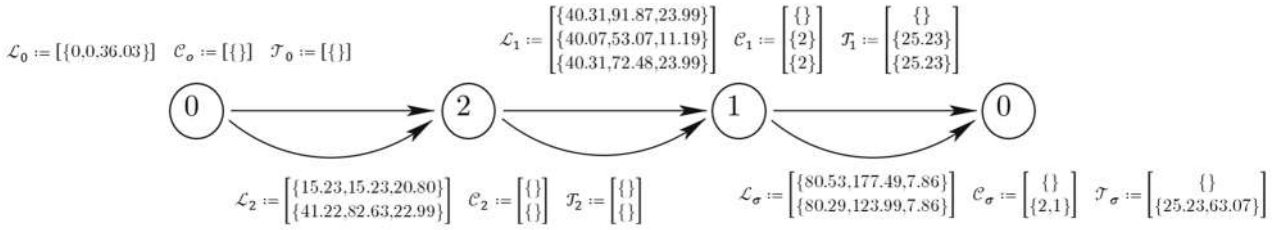

Figure 2 An illustrative example for the MG-DP

Note that the proposed MG-DP replaces the first stage DP in the DPIP algorithm used within the DP-ILNS algorithm proposed in Raeesi and Zografos (2020), and all other high-level features in our adoption of the DP-ILNS remain unchanged in MG-DP-ILNS (the second stage IP in the DPIP picks the optimal labels from the endpoint of the ECV routes to construct BSV routes). For brevity

we refer the reader to Raeesi and Zografos (2020) for further details regarding the ALG-III implementation of the DP-ILNS that we have used in the 'computational results' section of this paper. It is worth noting that with the proposed MG-DPIP we have in practice reduced the EVRPTW-RS-SMBS to the VRPTW on a multigraph, and hence any of the many successful algorithms for the VRPTWs could have been modified and used to tackle the problem.

5. Alternative business scenarios: cost and emissions implications

With the fast-paced developments in overcoming technoeconomic barriers in the face of material and equipment standardisation, and with the significant fall in lithium-ion battery packs price (80% fall since 2009, and another 50% expected fall from their current price by 2050 – Sanguesa et al., 2021), battery swapping is increasingly being recognised as a viable solution in the face of high adoption cost and limited driving range of electric vehicles (Bakogiannis, 2020), and is attracting influential proponents among EV leaders. NIO®, the Shanghai-based automaker, for example, officially launched the Battery as a Service (BaaS) option in August 2020, and has already completed over 800,000 swaps for BaaS users[1]. As patented by Gao et al. (2012) and Lu and Zhou (2013), and economically justified by the study of Shao et al. (2017), this service can be simply provided in a non-stationary mode via BSVs, which can be viewed as key accelerators for widespread adoption of EVs during the transition period.

Grasping an accurate idea of the viability of the proposed logistics model in this paper, on the other hand, requires a careful incorporation of the main cost and emissions components involved into the optimisation model and performing a reliable comparative analysis (with regard to economic and environmental objectives) against other viable business scenarios for operating on ECVs. In this section, we consider 4 logistics scenarios under two distinct objective functions: (i) the business objective pertaining to an aggregated function of the Total Cost of Ownership (TCO) and operational costs, and (ii) the environmental objective pertaining to the total amount of well-to-wheel CO_2 (in kg) emitted. These scenarios and their corresponding optimisation models are detailed next. In section 6 of the paper, we will use an urban and a regional case study in Greater London and Southeast England, respectively, to analyse the incurred costs and emissions of each of these business scenarios. It is worth mentioning that there are several other scenarios that could have been considered here (e.g., use of a third party company to provide BSV services), but these are beyond the scope of this study and require a rather dedicated analysis. We discuss some of these scenarios as important directions for future research in the 'discussion and conclusion' section of the paper.

5.1. Scenario I: ECVs and RSs

This is the baseline scenario. In this logistics scenario, there are no BSVs, and ECVs are only allowed to divert their delivery routes to visit privately owned RSs for recharging their batteries. The corresponding optimisation problem is a location-routing problem where routing ECVs is carried out simultaneously with deciding on the location of opened RSs among the potential sites.

The TCO component of the business objective function comprises the daily cost of an ECV (Ω_e) and the daily cost of an opened RS (Ω_r). Following related TCO approaches in the literature (Davis and Figliozzi, 2013; Lee et al., 2013; Feng and Figliozzi, 2013; Schiffer et al., 2017), Ω_e is calculated based on the purchase cost of the ECV, the battery replacement cost during the considered lifetime and the vehicle release value at the end of the lifetime. In the calculation of Ω_r, land lease/purchase cost, charger point cost, maintenance cost and cost of installation is considered for an equivalent lifetime of that of an ECV. The operational costs component of the business objective function, on the other hand, is calculated for each kilometre (km) travelled by an adopted ECV (ω_e) which includes maintenance and fuel cost per km travelled. Also, for the calculation of the environmental objective pertaining to the total amount of well-to-wheel CO_2 emitted, we use E_e to denote kg/km CO_2 emitted by an ECV.

To formulate and solve the problem under this scenario, the path-based formulation in Appendix D can be extended to include location decisions and disregard BSVs. To do this, let us define the binary input parameters $\Pi_{pi}, \forall p \in \mathcal{P}, i \in R$, which is 1 if path $p \in \mathcal{P}$ passes through RS $i \in R$ and zero, otherwise. We also define the binary variable $\mathcal{O}_i, \forall i \in R$ denoting whether RS $i \in R$ is opened or not. Then, the business objective function to replace objective functions (50) and (51) in the path-based formulation in Appendix D is the following:

$$Scenario\ I - Business\ Objective \coloneqq \Omega_e \sum_{(0,j,p)\in\mathcal{P}} x_{0jp} + \Omega_r \sum_{i\in R} \mathcal{O}_i + \omega_e \sum_{(i,j,p)\in\mathcal{P}} d_{ijp} x_{ijp} \tag{31}$$

And the environmental objective is expressed as follows:

$$Scenario\ I - Environmental\ Objective \coloneqq E_e \sum_{(i,j,p)\in\mathcal{P}} d_{ijp} x_{ijp} \tag{32}$$

[1] https://www.nio.com/news/nio-launches-battery-service

We also need to add the following constraints to the model:

$$\sum_{p\in\mathcal{P}} x_p \Pi_{pi} \leq M\mathcal{O}_i, \qquad \forall i \in R \tag{33}$$

$$\sum_{p\in\mathcal{P}} z_p = 0 \tag{34}$$

Constraints (33) determine if RS $i \in R$ is opened, and constraint (34) eliminates BSVs from the model. It is worth clarifying that in using x_p and z_p instead of x_{ijp} and z_{ijp} in constraints (33) and (34), we are taking advantage of the definition of the set $\mathcal{P}$ (i. e. , $\mathcal{P} = \bigcup_{i,j\in V_r} \mathcal{P}_{ij}$ in Theorem 1) as the ordered set of all paths.

5.2. Scenario II: ECVs and electric BSVs (eBSVs)

In this scenario, ECVs can extend their driving range by requesting battery swapping services from BSVs which are themselves operating on an electric battery (eBSVs). The company is assumed relying only on eBSVs and no RSs are opened. The corresponding optimisation problem is the EVRPTW-SMBS proposed in Raeesi and Zografos (2020).

The TCO component of the business objective function comprises the daily cost of an ECV (Ω_e), the daily cost of an eBSV (Ω_b) and the daily cost of each spare lithium-ion battery pack required (Ω_l). Ω_b can be calculated in the same fashion discussed for Ω_e, and Ω_l is calculated based on the purchasing cost of the battery pack divided by the total number of days in its lifetime. The operational costs component of the business objective function is calculated for each kilometre (km) travelled by an adopted ECV (ω_e) and eBSV (ω_b) based on maintenance and fuel cost per km travelled. Also, the same E_e factor is used to denote kg/km CO_2 emitted by an eBSV.

To formulate and solve the problem under this scenario, the path-based formulation in Appendix D can be modified to exclude RSs and used. The following business objective function should hence replace the objective functions (50) and (51) in the path-based formulation in Appendix D:

$$Scenario\ II - Business\ Objective \coloneqq \Omega_e \sum_{(0,j,p)\in\mathcal{P}} x_{0jp} + \Omega_b \sum_{(0,j,1)\in\mathcal{P}} z_{0j1} + \Omega_l \mathcal{B} + \omega_e \sum_{(i,j,p)\in\mathcal{P}} d_{ijp} x_{ijp} + \omega_b \sum_{(i,j,1)\in\mathcal{P}} d_{ij1} z_{ij1} \tag{35}$$

In this expression $\mathcal{B}$ denotes the total number of spare battery packs required.

The environmental objective is expressed as follows:

$$Scenario\ II - Environmental\ Objective \coloneqq \mathrm{E}_e\Big(\sum_{(i,j,p)\in\mathcal{P}} d_{ijp} x_{ijp} + \sum_{(i,j,1)\in\mathcal{P}} d_{ij1} z_{ij1}\Big) \tag{36}$$

We also need to add the following constraints to the model:

$$\mathcal{B} = \sum_{(i,j,1)\in\mathcal{P}:\, i\neq 0} z_{ij1} \tag{37}$$

$$\sum_{(i,j,p)\in\mathcal{P}:\, p>1} x_{ijp} = 0 \tag{38}$$

Constraint (37) determine the value of $\mathcal{B}$, and constraint (38) eliminates all refuelling paths from consideration. Remember that the first path in the set of paths between a pair of required nodes is the direct edge.

5.3. Scenario III: ECVs, eBSVs and RSs

In this scenario, ECVs can extend their driving range by either requesting battery swapping services from eBSVs or visiting privately owned RSs. The corresponding optimisation problem is the EVRPTW-RS-SMBS proposed in this paper.

The TCO component of the business objective function comprises the daily cost of an ECV (Ω_e), the daily cost of an eBSV (Ω_b), the daily cost of each spare lithium-ion battery pack required (Ω_l) and the daily cost of an opened RS (Ω_r). The operational costs component and the environmental factors are same as in Scenario II.

The following business objective function should replace the objective functions (50) and (51) in the path-based formulation in Appendix D:

$$Scenario\ III - Business\ Objective \coloneqq \Omega_e \sum_{(0,j,p)\in\mathcal{P}} x_{0jp} + \Omega_b \sum_{(0,j,1)\in\mathcal{P}} z_{0j1} + \Omega_l \mathcal{B} + \Omega_r \sum_{i\in R} \mathcal{O}_i + \omega_e \sum_{(i,j,p)\in\mathcal{P}} d_{ijp} x_{ijp} + \omega_b \sum_{(i,j,1)\in\mathcal{P}} d_{ij1} z_{ij1} \tag{39}$$

The environmental objective is as in expression (36). Also, note that constraints (33) are required.

5.3. Scenario IV: ECVs, internal combustion engine BSVs (iceBSVs) and RSs

In this scenario, we are interested in exploring the impact of using a conventionally fuelled BSV in supporting the routes of ECVs. Therefore, ECVs can extend their driving range by either requesting battery swapping services from Internal Combustion Engine BSVs (iceBSVs) or visiting privately owned RSs. The corresponding problem formulation and the business objective function remains similar to the case of Scenario III, and we only need to replace Ω_b and ω_b with $\Omega_b{}'$ and $\omega_b{}'$, respectively, and given that there is no range anxiety issue with iceBSVs, we need to set C_b at ∞.

As regards the environmental objective, we use E_ι to denote kg/km well-to-wheel CO_2 emitted by an iceBSV in the following expression:

$$Scenario\ IV - Environmental\ Objective \coloneqq \mathrm{E}_e \sum_{(i,j,p)\in\mathcal{P}} d_{ijp}x_{ijp} + \mathrm{E}_\iota \sum_{(i,j,1)\in\mathcal{P}} d_{ij1}z_{ij1} \tag{40}$$

The analysis of these scenarios in realistic case studies in the next section can contribute to deriving important managerial insights for goods distribution using ECVs.

6. Computational results and the case study

In this section, we first introduce a set of EVRPTW-RS-SMBS benchmark instances and use them to perform comparisons with the EVRPTW-RS and the EVRPTW-SMBS formulations and analyse the performance of the proposed path-based formulation and the heuristic algorithm. Then, the case study is presented to analyse the alternative business scenarios discussed in section 5 of the paper.

All tests were conducted on a computer with Intel Core™ i7 2.50 GHz processor with 8 GB RAM. The branch-and-bound solver of CPLEX™ 12.10 was used as the exact solver, and all other algorithms were coded in MATLAB R2020a™. Whenever needed, CPLEX™ is called from MATLAB™.

6.1. Generation of EVRPTW-RS-SMBS test instances

We derive new EVRPTW-RS-SMBS test instances from the EVRPTW instances proposed by Schneider et al. (2014), which are based on the well-known Solomon (1987) benchmark instances for the VRPTW. Since in Schneider et al. (2014) solutions are purely based on intra-route recharging, the detours for visits to RSs and the resulting recharging times make it impossible to comply with the customer time windows given in the original Solomon (1987) instances. Therefore, Schneider et al. (2014) generate new time-windows to obtain feasible EVRPTW-RS instances. This, however, is not a limitation for the proposed problem variant in this paper, as it is always possible to find a feasible solution if the given instance itself is feasible. Therefore, we apply two main modifications corresponding to using the original time-windows of Solomon (1987) instances instead of the ones generated by Schneider et al. (2014), and increasing the value for the inverse recharging rates used in their study. These simple modifications make the problems particularly harder to solve and would better highlight the added value of the EVRPTW-RS-SMBS. The BSV characteristics (i.e., Q_b, C_b, and r_b) used in our experiments, on the other hand, are adopted directly from Raeesi and Zografos (2020). Instances of sizes 5, 10, 15, 25, and 100 customers are generated, where instances with 25 and 100 customer locations comprise 21 RS locations. All the test instances developed in this paper along with the details of the reported solutions in this section, and a supplementary document for the detailed tables of the results are all available at https://data.kent.ac.uk/400/.

6.2. The added value of the EVRPTW-RS-SMBS

In order to demonstrate the added value of the EVRPTW-RS-SMBS, all test instances are solved under three different settings: (i) the EVRPTW-RS-SMBS, (ii) the EVRPTW-SMBS and (iii) the EVRPTW-RS. Corresponding path-based formulations of instances with 5, 10, 15 and 25 customers are put into CPLEX, and instances with 100 customers are solved heuristically using appropriate variations of the proposed MG-DP-ILNS algorithm. The branch-and-bound solver of CPLEX is given a maximum of 7200 seconds for each instance, and an optimal or near optimal solution is returned upon this termination criterion. As the EVRPTW-SMBS and the EVRPTW-RS are special cases of the EVRPTW-RS-SMBS, the proposed MG-DP-ILNS have been slightly modified and used in the case of each instance with 100 customers. All parameters used within the MG-DP-ILNS are adopted from Raeesi and Zografos (2020) and all algorithms were run 10 times on each instance, and the best result is returned. A summary of the results from the conducted experiments are presented in Table 1 to Table **3**.

In Table 1, the aggregated results of the experiments on instances with 5, 10 and 15 customers are presented. The given headings in this table and other tables in this section denote the following:

- V_E: total number of ECVs used in the solution.

- D_E: total distance travelled by ECVs.
- V_B: total number of BSVs used in the solution.
- D_B: total distance travelled by BSVs.
- S: total number of battery swaps requested.
- V_T: total number of vehicles (ECVs and BSVs) used in the solution.
- D_T: total distance travelled by all vehicles (ECVs and BSVs).

The values under each heading are the averages of the optimal or near optimal solutions found to instances in each group under the given setting. If for a given instance under a given setting no feasible solution has been found after the permitted CPU time, the corresponding instance has been excluded from the averages calculations for all settings. In total one of the 15-customer instances is excluded on this basis as CPLEX was unable to solve it under the setting of the EVRPTW-SMBS after the permitted CPU time of 7200 seconds. The detailed solutions to all instances under all settings with the MIP gaps are reported in the online supplementary document in Table SD.1.

Note that each instance is first solved for the minimisation of the objective function corresponding to the total number of ECVs and BSVs required, and then the total distance for the minimum number of vehicles found is minimised. Therefore, in all cases a solution with a smaller value for V_T is preferred.

Table 1
Aggregated results of the experiments on instances with 5, 10 and 15 customers

Instant size	Problem type	V_E	D_E	V_B	D_B	S	V_T	D_T
	EVRPTW-RS-SMBS	1.92	201.77	0.08	4.96	0.08	**2.00**	206.73
$n = 5$	EVRPTW-SMBS	1.58	188.20	1.17	103.05	2.08	2.75	291.25
	EVRPTW-RS	2.08	205.25	0.00	0.00	0.00	2.08	205.25
	EVRPTW-RS-SMBS	2.50	301.35	0.25	24.27	0.58	**2.75**	325.61
$n = 10$	EVRPTW-SMBS	2.17	281.63	1.42	133.98	3.50	3.58	415.61
	EVRPTW-RS	2.92	317.40	0.00	0.00	0.00	2.92	317.40
	EVRPTW-RS-SMBS	3.00	375.10	0.25	26.55	0.75	**3.25**	401.65
$n = 15$	EVRPTW-SMBS	2.64	336.19	1.45	147.42	3.82	4.09	483.62
	EVRPTW-RS	3.58	384.21	0.00	0.00	0.00	3.58	384.21

Table 1 shows that despite the use of BSVs alongside visits to RSs, the total number of vehicles required (i.e., V_T) in the case of the EVRPTW-RS-SMBS is always smaller than that of the EVRPTW-SMBS which is reluctant to visits to RSs, and the EVRPTW-RS which does not use BSVs to support the routes of running ECVs. Also note that in most cases solutions from the EVRPTW-RS are preferred over the solutions from the EVRPTW-SMBS. This is, however, the opposite in the case of the large sized instances which will be discussed further shortly. As expected also, the number of ECVs required is smallest in the case of the EVRPTW-SMBS and largest in the case of the EVRPTW-RS.

Similar results are presented for instances with 25 and 100 customers and 21 RSs in Table 2 and Table **3**, respectively. In these tables, aggregated results are presented for instances in each of the six sets of C1, C2, R1, R2, RC1 and RC2, and as averages over all the 56 instances considered.

Table 2 shows again that the best results are obtained under the setting of the EVRPTW-RS-SMBS. From all the 56 instances of size 25 considered, 47 instances were included in calculating the averages presented in the table as no solutions were found for some of the instances under some of the settings within the permitted CPU time. Detailed results for all instances under all settings with the MIP gaps are reported in the online supplementary document in Table SD.2. Note again that except for instances in group C1, the EVRPTW-RS setting provides a better solution than the EVRPTW-SMBS. Furthermore, an interesting result presented in Table 2 corresponds to the similarity between the solutions from the EVRPTW-RS-SMBS and the EVRPTW-RS in case of the instances in group 2; i.e., C2, R2, and RC2. In Solomon (1987) instances, problem sets in the first group (i.e., R1, C1, and RC1) have a short scheduling horizon, whereas the second group instances (i.e., R2, C2, and RC2) have a longer scheduling horizon. As time windows are not very tight in instances of group 2, there is not much time pressure to satisfy customers' time windows and the time required for visits to RSs is not much restrictive; thus, recharging at RSs is preferred over calling for a battery swapping service from a BSV. In cases where the EVRPTW-RS-SMBS is using BSVs to extend the driving range of running ECVs, compared with the EVRPTW-SMBS, very few BSVs are employed to travel a rather short distance and very few fully charged batteries are required.

Table 2
Aggregated results of the experiments on instances with 25 customers

Instant group	Problem type	V_E	D_E	V_B	D_B	S	V_T	D_T
	EVRPTW-RS-SMBS	4.86	529.33	0.86	85.28	2.71	**5.71**	614.61
C1	EVRPTW-SMBS	4.43	518.34	1.71	139.68	4.71	6.14	658.02
	EVRPTW-RS	7.00	621.09	0.00	0.00	0.00	7.00	621.09
	EVRPTW-RS-SMBS	2.57	409.09	0.00	0.00	0.00	**2.57**	409.09
C2	EVRPTW-SMBS	2.29	414.33	1.00	82.16	2.29	3.29	496.49
	EVRPTW-RS	2.57	409.09	0.00	0.00	0.00	**2.57**	409.09
	EVRPTW-RS-SMBS	6.63	534.47	0.38	20.33	0.88	**7.00**	554.80
R1	EVRPTW-SMBS	5.63	494.04	1.88	161.19	5.63	7.50	655.23
	EVRPTW-RS	7.13	552.45	0.00	0.00	0.00	7.13	552.45
	EVRPTW-RS-SMBS	2.00	385.24	0.00	0.00	0.00	**2.00**	385.24
R2	EVRPTW-SMBS	2.64	373.67	0.00	0.00	0.00	2.64	373.67
	EVRPTW-RS	2.00	385.24	0.00	0.00	0.00	**2.00**	385.24
	EVRPTW-RS-SMBS	6.67	663.79	0.17	25.04	0.67	**6.83**	688.83
RC1	EVRPTW-SMBS	5.33	614.88	2.00	211.47	6.33	7.33	826.35
	EVRPTW-RS	7.17	683.29	0.00	0.00	0.00	7.17	683.29
	EVRPTW-RS-SMBS	2.25	533.09	0.00	0.00	0.00	**2.25**	533.09
RC2	EVRPTW-SMBS	2.75	534.02	0.25	16.50	0.63	3.00	550.52
	EVRPTW-RS	2.25	533.24	0.00	0.00	0.00	**2.25**	533.24
	EVRPTW-RS-SMBS	3.94	496.38	0.21	19.36	0.64	**4.15**	515.74
All	EVRPTW-SMBS	3.72	479.85	1.02	90.28	2.91	4.74	570.13
	EVRPTW-RS	4.40	515.62	0.00	0.00	0.00	4.40	515.62

Table 3 shows results for instances with 100 customers and 21 RSs. It is observed that 6 out of the 56 instances with 100 customers (mostly in the set C1) are infeasible under the EVRPTW-RS setting (see details of all results under all setting in the online supplementary document in Tables SD.3 to SD.5) and these instances are excluded from averages calculations. This highlights a key argument in Raeesi and Zografos (2020) corresponding to a shortcoming of EVRPTW-RS in designing energy-feasible ECV routes when customers' time windows are tight, and the large refuelling time required at RSs is prohibitive. It is also observed that unlike all previous cases for 5, 10, 15 and 25 customers, in the case of the large test instances with 100 customers, solutions yielded by the EVRPTW-SMBS are more favourable than the solutions based on the EVRPTW-RS. EVRPTW-RS solutions are particularly costly to implement in the case of 100-customer instances. This is in line with the findings from Raeesi and Zografos (2020) that argue in larger sized test instances the use of BSVs is particularly beneficial over visiting RSs as the utilisation rate of BSVs increases in these instances. Finally, we observe that similar to previous tables, instances in groups R2 and RC2 are better off without requesting a battery swapping service.

Table 3
Aggregated results of the experiments on instances with 100 customers

Instant group	Problem type	V_E	D_E	V_B	D_B	S	V_T	D_T
	EVRPTW-RS-SMBS	10.25	869.05	2.00	214.30	4.75	**12.25**	1083.35
C1	EVRPTW-SMBS	10.50	970.77	2.25	261.49	7.00	12.75	1232.26
	EVRPTW-RS	16.25	1476.66	0.00	0.00	0.00	16.25	1476.66
	EVRPTW-RS-SMBS	4.00	696.27	0.75	43.05	1.13	**4.75**	739.33
C2	EVRPTW-SMBS	4.13	661.16	1.00	138.23	3.63	5.13	799.39
	EVRPTW-RS	5.88	1128.32	0.00	0.00	0.00	5.88	1128.32
	EVRPTW-RS-SMBS	16.33	1349.83	2.17	204.83	7.67	**18.50**	1554.66
R1	EVRPTW-SMBS	16.50	1358.41	3.33	317.27	12.92	19.83	1675.68
	EVRPTW-RS	21.17	1860.82	0.00	0.00	0.00	21.17	1860.82

	EVRPTW-RS-SMBS	4.36	992.14	0.00	0.00	0.00	**4.36**	992.14
R2	EVRPTW-SMBS	4.55	942.26	0.55	29.96	1.82	5.09	972.23
	EVRPTW-RS	4.36	987.63	0.00	0.00	0.00	**4.36**	987.63
	EVRPTW-RS-SMBS	15.43	1512.49	1.71	206.14	6.43	**17.14**	1718.62
RC1	EVRPTW-SMBS	15.29	1485.81	3.00	368.29	11.86	18.29	1854.10
	EVRPTW-RS	19.71	1969.60	0.00	0.00	0.00	19.71	1969.60
	EVRPTW-RS-SMBS	4.88	1094.56	0.00	0.00	0.00	**4.88**	1094.56
RC2	EVRPTW-SMBS	4.88	1144.71	0.88	65.22	2.88	5.75	1209.93
	EVRPTW-RS	4.88	1094.56	0.00	0.00	0.00	**4.88**	1094.56
	EVRPTW-RS-SMBS	9.28	1110.04	1.04	102.05	3.30	**10.32**	1212.09
All	EVRPTW-SMBS	9.38	1107.93	1.82	187.77	6.76	11.20	1295.70
	EVRPTW-RS	11.82	1413.41	0.00	0.00	0.00	11.82	1413.41

The aggregated results for all 100-customer instances indicate that on average each BSV can support the routes of 8 ECVs in the case of the EVRPTW-RS-SMBS. This, alongside visits to RSs for stationary intra-route recharging, provides a significant opportunity for facilitating goods distribution using ECVs.

Next, we present several computational results to demonstrate the performance of the proposed NDPI algorithm and the path-based formulation of the EVRPTW-RS-SMBS and its related problem class, i.e., the EVRPTW-RS.

6.3. The performance of the NDPI algorithm and the path-based formulation

To begin with the evaluation of the proposed NDPI algorithm, we initially solve EVRPTW-RS-SMBS instances of size 5, 10 and 15 to optimality (or near optimality) using the original formulation of the problem given in (1)-(26), and the path-based formulation in (50)-(75), and compare the performance of the two. Note that the original formulation is unable to handle any of the instances with 25 customers and 21 RSs as size of the enumeration tree in the MIP solver increases exponentially with the number of binary variables required for representing the dummy copies of the RSs. On the other hand, as reported in the previous section, the path-based formulation is able to find optimal or feasible solutions to 48 instances out of the 56 instances considered in this set. We have given the solver a maximum of 7200 seconds for each instance of size 5, 10 and 15 and all results are reported in Table 4. The table shows the obtained values for V_T and D_T in the case of the original and the path-based formulation of the EVRPTW-RS-SMBS, as well as the total computing time (t) in seconds (s) for the minimisation of the total distance of ECVs and BSVs after the first objective has been minimised, and the MIP gap at the termination of the solver. Also, under the path-based formulation, the average number of nondominated paths identified between every pair of required nodes (including the direct edge) is given under the column with 'Avg. paths' heading. Note that, we have not included the NDPI pre-processing time as this is negligible across all instances considered.

Table 4
Comparison of the original formulation for the EVRPTW-RS-SMBS with the path-based formulation

No.	Inst.	Original formulation				Path-based formulation				
		V_T	D_T	t (s)	MIP gap	Avg. paths	V_T	D_T	t (s)	MIP gap
1	C101-5	4	313.84	0.23	0.00	1.80	4	313.84	0.08	0.00
2	C103-5	2	154.50	0.09	0.00	3.10	2	154.50	0.06	0.00
3	C206-5	1	214.36	0.13	0.00	3.65	1	214.36	0.03	0.00
4	C208-5	1	180.96	2.23	0.00	3.40	1	180.96	0.27	0.00
5	R104-5	3	161.25	0.13	0.00	3.90	3	161.25	0.08	0.00
6	R105-5	3	182.92	0.13	0.00	2.40	3	182.92	0.05	0.00
7	R202-5	1	128.78	0.08	0.00	4.25	1	128.78	0.08	0.00
8	R203-5	1	242.41	5.95	0.00	4.40	1	242.41	0.38	0.00
9	RC105-5	3	238.05	0.08	0.00	2.00	3	238.05	0.06	0.00
10	RC108-5	3	316.51	0.45	0.00	3.00	3	316.51	0.11	0.00
11	RC204-5	1	176.39	0.28	0.00	5.05	1	176.39	0.31	0.00
12	RC208-5	1	167.98	0.16	0.00	4.70	1	167.98	0.17	0.00

13	C101-10	4	527.52	0.66	0.00	1.83	4	527.52	0.09	0.00
14	C104-10	2	332.87	2313.85	0.00	4.54	2	332.87	1256.17	0.00
15	C202-10	2	264.76	1.06	0.00	3.10	2	264.76	0.42	0.00
16	C205-10	2	228.28	0.90	0.00	2.59	2	228.28	0.20	0.00
17	R102-10	4	284.67	4.78	0.00	2.49	4	284.67	1.95	0.00
18	R103-10	3	211.24	17.86	0.00	3.31	3	211.24	23.00	0.00
19	R201-10	*1*	*300.317*	*7200.00*	*0.28*	3.02	1	292.78	0.13	0.00
20	R203-10	2	232.68	2.11	0.00	4.83	2	232.68	0.97	0.00
21	RC102-10	5	429.15	0.31	0.00	1.78	5	429.15	0.13	0.00
22	RC108-10	4	396.22	58.91	0.00	2.59	4	396.22	7.3	0.00
23	RC201-10	2	313.65	2.13	0.00	3.13	2	313.65	0.22	0.00
24	RC205-10	2	393.55	6.77	0.00	2.92	2	393.55	0.45	0.00
25	C103-15	-*	-	*7200.00*	-	3.66	*3*	*516.78*	*7200.00*	*0.35*
26	C106-15	4	393.04	49.96	0.10	1.87	4	393.04	1.70	0.00
27	C202-15	3	384.80	2.7	0.00	3.28	3	384.80	0.81	0.00
28	C208-15	2	287.42	1.06	0.00	2.84	2	287.42	0.92	0.00
29	R102-15	*4*	*362.05*	*7200.00*	*0.25*	3.89	4	362.05	234.81	0.00
30	R105-15	5	446.96	262.94	0.00	2.00	5	446.96	3.00	0.00
31	R202-15	*3*	*488.58*	*7200.00*	*0.26*	3.86	3	409.04	33.30	0.00
32	R209-15	*2*	*338.54*	*7200.00*	*0.09*	4.38	2	338.54	1081.78	0.00
33	RC103-15	5	469.67	15.39	0.00	2.33	5	469.67	11.36	0.00
34	RC108-15	*5*	*467.58*	*7200.00*	*0.31*	2.63	5	467.58	1756.95	0.09
35	RC202-15	*2*	*381.44*	*7200.00*	*0.20*	4.05	2	381.44	193.08	0.00
36	RC204-15	-	-	*7200.00*	-	6.20	*1*	*353.56*	*7200*	*0.18*

* No feasible solution has been found after the permitted computational time

It can be observed in Table 4 that the runtime of the path-based formulation of the EVRPTW-RS-SMBS is significantly smaller than that of the original formulation in most cases. The path-based formulation is able to find the optimal solution to all instances considered, except for instances C103-15 and RC204-15 (shown in *italic*); however, the original formulation fails to close the MIP gap within the permitted time in the case of 6 instances and is unable to find any feasible solution to two of the instances, i.e., C103-15, and RC204-15.

Since the results presented in this paper are generalisable to other related problem classes (e.g., the EVRPTW-RS and the Green-VRP), to investigate further the effectiveness of the proposed algorithm for the identification of nondominated paths, we concentrate also on the EVRPTW-RS, which is a special case of the EVRPTW-RS-SMBS. Here, we demonstrate that by just putting a path-based formulation of the EVRPTW-RS into CPLEX, it is possible to obtain results that are well comparable with the results from a sophisticated branch-price-and-cut algorithm proposed by Desaulniers et al. (2016) for the EVRPTW-RS. The path-based formulation has also the added value of improving several of the solutions found by Desaulniers et al. (2016) in terms of the total number of ECVs required (the algorithm proposed by Desaulniers et al. (2016) does not minimise the total number of ECVs), and putting forth upper bounds to several of the previously unsolved instances. In Desaulniers et al. (2016) four variants of the EVRPTW-RS resulting from the combination of the adopted recharging strategy (i.e., full or partial) and recharging frequency (single or multiple recharge per route) are considered and for each variant, an exact branch-price-and-cut algorithms is presented. They mainly concentrate on the first group of test problems developed by Schneider et al. (2014) (i.e., test sets R1, C1, and RC1), which are characterized by narrow time windows, and show that they can solve instances with up to 100 customers and 21 recharging stations. We also use the same set of 25, 50 and 100 test instances they use and show that the path-based formulation can handle many of them. Note that the path-based formulation can tackle the second variant of the EVRPTW-RS they consider, i.e., multiple recharges per route, with full recharges only. Similar to their study, we have applied a maximum computational time of 3600 s on CPLEX.

The result of this comparison is presented in Table 5. In this table, upper bounds obtained using the path-based formulation are compared with those reported by Desaulniers et al. (2016) (under the heading Des. et al.) for EVRPTW instances with 25, 50 and 100 customers and 21 RSs. Path-based solutions in *italic* are matching with Des. et al. solutions, and solutions in **bold** are improving their solutions. Note again that Desaulniers et al. (2016) do not consider the minimisation of the number of vehicles

needed, and hence the improvements are either in the total number of ECVs required, or they are upper bounds to problems that had remained unsolved using the branch-price and-cut algorithm of Desaulniers et al. (2016).

Table 5
The path-based formulation for the EVRPTW-RS instances with 25, 50 and 100 customers and 21 RSs

Inst.	25 customers 21 RSs				50 customers 21 RSs				100 customers 21 RSs			
	Des. et al.		Path-based		Des. et al.		Path-based		Des. et al.		Path-based	
	V_E	D_E	V_E	D_E	V_E	D_E	V_E	D_E	V_E	D_E	V_E	D_E
C101	7	626.9	**5**	**708.9**	9	783.6	**7**	**904.7**	12	1053.8	12	1094.0
C102	5	526.2	*5*	*526.2*	8	784.7	9	788.4	12	1022.6	-	-
C103	4	345.4	*4*	*345.4*	7	656.7	7	677.4	-	-	-	-
C104	*4*	*449.8*	*4*	*449.8*	*5*	*582.7*	*6*	*600.0*	-	-	***13***	***1226.2***
C105	6	541.4	**4**	**620.1**	9	736.8	**8**	**777.6**	12	1033.9	12	1062.4
C106	5	562.3	**4**	**619.4**	9	755.0	9	764.0	12	1027.3	-	-
C107	6	505.7	**4**	**629.0**	7	708.7	*7*	*708.7*	12	1025.6	-	-
C108	5	508.3	*5*	*508.3*	8	726.0	*8*	*726.0*	-	-	-	-
C109	4	473.4	4	475.4	7	677.0	7	686.4	-	-	**12**	**1030.1**
R101	*9*	*662.2*	*9*	*662.2*	*12*	*939.9*	***11***	***961.8***	*20*	*1601.8*	***18***	***1639.9***
R102	6	452.9	**5**	**470.2**	10	866.7	-	-	18	1454.9	-	-
R103	6	494.5	*6*	*494.5*	9	803.2	10	819.0	-	-	**17**	**1350.6**
R104	4	352.0	*4*	*352.0*	-	-	**7**	**633.6**	-	-	**14**	**1254.8**
R105	6	584.4	*6*	*584.4*	10	842.4	*10*	*842.4*	15	1340.2	-	-
R106	5	480.1	*5*	*480.1*	9	794.0	9	797.6	14	1229.2	-	-
R107	5	416.3	5	417.2	8	691.4	-	-	-	-	**17**	**1422.1**
R108	4	429.2	-	-	6	543.5	7	585.0	-	-	**14**	**1251.2**
R109	5	462.1	*5*	*462.1*	8	789.4	-	-	-	-	-	-
R110	4	419.5	4	427.2	7	713.4	-	-	-	-	-	-
R111	4	382.9	*4*	*382.9*	7	745.1	-	-	-	-	**16**	**1336.8**
R112	4	397.2	*4*	*397.2*	6	602.8	7	659.1	-	-	**15**	**1352.2**
RC101	7	738.0	**6**	**791.6**	11	1074.1	*11*	*1074.1*	-	-	**17**	**1706.2**
RC102	7	648.3	7	649.3	10	897.2	10	922.8	16	1531.8	-	-
RC103	6	560.7	*6*	*560.7*	8	829.4	9	873.3	-	-	-	-
RC104	4	516.3	*4*	*516.3*	7	690.0	7	694.0	-	-	**14**	**1465.8**
RC105	6	589.7	*6*	*589.7*	10	983.9	-	-	15	1482.2	16	1650.6
RC106	5	557.1	*5*	*557.1*	8	888.0	9	911.9	-	-	-	-
RC107	4	497.5	*4*	*497.5*	7	786.2	8	811.8	-	-	-	-
RC108	4	479.6	*4*	*479.6*	-	-	**7**	**751.4**	-	-	-	-

6.4. The performance of the heuristic algorithm

In order to evaluate the performance of the proposed heuristic for the EVRPTW-RS-SMBS, the optimal and near optimal solutions found to instances with 5, 10, 15 and 25 customers in previous sections are compared with the solutions found by the MG-DP-ILNS. These comparisons are presented in Table 6 and Table 7. Table 6 compares the solutions yielded by the MG-DP-ILNS with the solutions from the path-based formulation for instances with 5, 10 and 15 customers, and Table 7 does so for instances with 25 customers and 21 RSs. In these tables, t (s) is the average computing time (CPU) in seconds over ten runs. The 'Gap1' column reports the percentage gap between the V_T form the path-based solution ($V_{T(1)}$) with the V_T form the MG-DP-ILN solution ($V_{T(2)}$). This is calculated as follows for each instance: $[(V_{T(2)})- (V_{T(1)})]/ (V_{T(1)})$. Column 'Gap2' does so for the D_Ts form each method. Any negative gap reported in 'Gap1' and 'Gap2' columns is due to the suboptimality of the solution returned by the path-based formulation after 7200 seconds.

Table 6
Comparison of the MG-DP-ILNS solutions with the solutions from the path-based formulation for the EVRPTW-RS-SMBS instances with 5, 10 and 15 customers

No.	Inst.	Path-based formulation			MG-DP-ILNS				
		V_T	D_T	t (s)	V_T	D_T	t (s)	Gap1	Gap2
1	C101-5	4	313.84	0.08	4	313.84	0.04	0.00	0.00
2	C103-5	2	154.50	0.06	2	154.50	0.20	0.00	0.00
3	C206-5	1	214.36	0.03	1	214.36	0.10	0.00	0.00
4	C208-5	1	180.96	0.27	1	180.96	0.03	0.00	0.00
5	R104-5	3	161.25	0.08	3	161.25	0.13	0.00	0.00
6	R105-5	3	182.92	0.05	3	182.92	0.08	0.00	0.00
7	R202-5	1	128.78	0.08	1	128.78	0.06	0.00	0.00
8	R203-5	1	242.41	0.38	1	242.41	0.14	0.00	0.00
9	RC105-5	3	238.05	0.06	3	238.05	0.56	0.00	0.00
10	RC108-5	3	316.51	0.11	3	316.51	0.39	0.00	0.00
11	RC204-5	1	176.39	0.31	1	179.16	0.04	0.00	0.02
12	RC208-5	1	167.98	0.17	1	167.98	0.11	0.00	0.00
13	C101-10	4	527.52	0.09	4	527.52	0.13	0.00	0.00
14	C104-10	2	332.87	1256.17	2	332.87	0.62	0.00	0.00
15	C202-10	2	264.76	0.42	2	264.76	0.50	0.00	0.00
16	C205-10	2	228.28	0.20	2	228.28	0.87	0.00	0.00
17	R102-10	4	284.67	1.95	4	286.82	0.45	0.00	0.01
18	R103-10	3	211.24	23.00	3	215.52	0.29	0.00	0.02
19	R201-10	1	292.78	0.13	1	292.78	1.33	0.00	0.00
20	R203-10	2	232.68	0.97	2	232.68	0.73	0.00	0.00
21	RC102-10	5	429.15	0.13	5	429.15	0.48	0.00	0.00
22	RC108-10	4	396.22	7.3	4	396.22	0.32	0.00	0.00
23	RC201-10	2	313.65	0.22	2	313.65	0.42	0.00	0.00
24	RC205-10	2	393.55	0.45	2	393.55	0.20	0.00	0.00
25	C103-15	*3*	*516.78*	*7200.00*	3	516.779	0.92	0.00	0.00
26	C106-15	4	393.04	1.70	4	393.04	1.40	0.00	0.00
27	C202-15	3	384.80	0.81	3	384.80	1.93	0.00	0.00
28	C208-15	2	287.42	0.92	2	287.42	3.52	0.00	0.00
29	R102-15	4	362.05	234.81	4	362.05	2.22	0.00	0.00
30	R105-15	5	446.96	3.00	5	446.96	0.26	0.00	0.00
31	R202-15	3	409.04	33.30	3	417.95	3.34	0.00	0.02
32	R209-15	2	338.54	1081.78	2	338.54	13.53	0.00	0.00
33	RC103-15	5	469.67	11.36	5	469.67	1.50	0.00	0.00
34	RC108-15	5	467.58	1756.95	5	470.74	2.31	0.00	0.01
35	RC202-15	2	381.44	193.08	2	381.44	7.78	0.00	0.00
36	RC204-15	*1*	*353.56*	*7200.00*	1	353.56	58.43	0.00	0.00

Table 6 shows that except for five cases where the D_T of the solution returned by the MG-DP-ILNS has a gap of less than 2% from the optimal (near-optimal) solution by the path-based formulation, in all other cases the solutions are exactly matched.

In Table 7, these results are presented for instances with 25 customers and 21 RSs. The table shows that no feasible solution has been found to 8 of the instances approached by the path-based formulation of the EVRPTW-RS-SMBS, and the italic entries indicate a sub-optimal solution returned after 7200 seconds. The table clearly indicates the favourable performance of the proposed algorithm, which is exactly matching most of the optimal solutions and improving several of the sub-optimal ones.

Table 7
Comparison of the MG-DP-ILNS solutions with the solutions from the path-based formulation for EVRPTW-RS-SMBS instances with 25 customers

No.	Inst.	Path-based formulation			DP-ILNS				
		V_T	D_T	t (s)	V_T	D_T	t (s)	Gap1	Gap2
1	C101-25	7	742.36	10.94	7	749.82	157.43	0.00	0.01
2	C102-25	*6*	*673.16*	*7200.00*	6	673.16	101.36	0.00	0.00
3	C103-25	*5*	*451.42*	*7200.00*	4	511.61	83.23	-0.20	0.13
4	C104-25	-	-	7200.00	4	575.13	245.62	-	-
5	C105-25	6	700.84	3017.29	6	700.84	229.54	0.00	0.00
6	C106-25	6	635.47	188.57	6	635.47	234.16	0.00	0.00
7	C107-25	5	680.68	1750.95	5	680.68	107.62	0.00	0.00
8	C108-25	6	526.23	30.70	5	606.60	171.81	-0.17	0.15
9	C109-25	*5*	*565.27*	*7200.00*	5	565.27	74.26	0.00	0.00
10	C201-25	3	395.89	0.49	3	395.89	252.49	0.00	0.00
11	C202-25	3	408.42	19.23	2	531.91	114.72	-0.33	0.30
12	C203-25	3	428.89	462.36	2	464.57	129.95	-0.33	0.08
13	C204-25	2	342.49	6639.97	2	342.49	162.90	0.00	0.00
14	C205-25	2	430.81	3.94	2	430.81	164.66	0.00	0.00
15	C206-25	-	-	7200.00	2	520.67	150.64	-	-
16	C207-25	2	446.40	326.59	2	446.40	68.92	0.00	0.00
17	C208-25	3	410.71	2.72	2	488.80	103.02	-0.33	0.19
18	R101-25	9	733.95	1.54	9	733.95	306.50	0.00	0.00
19	R102-25	*9*	*607.35*	*7200.00*	9	612.00	382.03	0.00	0.01
20	R103-25	-	-	7200.00	6	461.15	230.37	-	-
21	R104-25	*5*	*394.77*	*7200.00*	5	395.49	288.72	0.00	0.00
22	R105-25	*7*	*701.03*	*7200.00*	7	701.03	70.84	0.00	0.00
23	R106-25	*7*	*532.54*	*7200.00*	7	532.54	681.23	0.00	0.00
24	R107-25	*6*	*435.66*	*7200.00*	6	435.66	250.27	0.00	0.00
25	R108-25	*6*	*502.95*	*7200.00*	6	511.70	247.98	0.00	0.02
26	R109-25	7	530.15	6757.21	7	530.15	121.41	0.00	0.00
27	R110-25	-	-	7200.00	6	494.35	217.65	-	-
28	R111-25	-	-	7200.00	6	503.21	289.78	-	-
29	R112-25	-	-	7200.00	5	423.43	167.85	-	-
30	R201-25	2	434.49	10.53	2	434.49	71.57	0.00	0.00
31	R202-25	2	477.91	155.19	2	480.32	97.67	0.00	0.01
32	R203-25	*2*	*465.73*	*7200.00*	2	461.61	132.72	0.00	-0.01
33	R204-25	*2*	*306.89*	*7200.00*	1	311.07	107.05	-0.50	0.01
34	R205-25	2	411.87	24.95	2	412.67	57.16	0.00	0.00
35	R206-25	2	391.50	707.15	2	391.50	141.60	0.00	0.00
36	R207-25	2	340.55	2643.52	2	340.55	224.72	0.00	0.00
37	R208-25	2	306.38	2302.35	2	306.38	43.93	0.00	0.00
38	R209-25	2	399.01	118.44	2	399.01	74.01	0.00	0.00
39	R210-25	2	334.43	217.63	2	334.43	70.11	0.00	0.00
40	R211-25	*2*	*368.92*	*7200.00*	1	406.07	66.73	-0.50	0.10
41	RC101-25	7	878.72	2190.40	7	878.72	477.08	0.00	0.00
42	RC102-25	8	747.90	6577.33	8	747.90	265.36	0.00	0.00
43	RC103-25	*5*	*528.98*	*7200.00*	5	528.98	500.64	0.00	0.00
44	RC104-25	*7*	*674.54*	*7200.00*	7	674.54	153.72	0.00	0.00
45	RC105-25	7	665.35	5852.55	7	665.35	152.04	0.00	0.00

46	RC106-25	7	637.48	160.51	7	637.48	307.13	0.00	0.00
47	RC107-25	-	-	7200.00	6	671.80	184.57	-	-
48	RC108-25	-	-	7200.00	6	582.06	268.76	-	-
49	RC201-25	2	733.54	25.37	2	738.04	457.51	0.00	0.01
50	RC202-25	*2*	*568.59*	*7200.00*	2	568.59	434.58	0.00	0.00
51	RC203-25	*2*	*499.17*	*7200.00*	2	499.17	365.76	0.00	0.00
52	RC204-25	*2*	*400.77*	*7200.00*	2	400.77	45.74	0.00	0.00
53	RC205-25	2	611.26	92.49	2	611.26	144.69	0.00	0.00
54	RC206-25	3	538.02	66.97	2	575.14	92.37	-0.33	0.07
55	RC207-25	3	473.78	4844.12	2	490.98	135.86	-0.33	0.04
56	RC208-25	*2*	*439.62*	*7200.00*	2	439.62	96.78	0.00	0.00

Finally, in Table 8 we are presenting detailed results for EVRPTW-RS-SMBS instances with 100 customers and 21 RSs. The table shows the efficiency of the proposed algorithm in solving a considerably challenging problem, where alongside with the ECVs visits to RSs, very few BSVs are required to support the routes of multiple ECVs.

Table 8

DP-ILNS results for EVRPTW-RS-SMBS instances with 100 customers and 21 RSs

No.	Inst.	V_E	D_E	V_B	D_B	S	V_T	D_T	t (s)
1	C101-100	10	828.94	2	265.50	5	12	1094.44	980.67
2	C102-100	10	828.94	2	265.50	5	12	1094.44	575.75
3	C103-100	10	823.46	2	230.97	5	12	1054.43	1213.50
4	C104-100	10	851.36	2	176.33	4	12	1027.69	1714.00
5	C105-100	10	830.46	2	262.98	5	12	1093.44	2953.29
6	C106-100	10	828.94	2	265.50	5	12	1094.44	798.42
7	C107-100	10	827.55	2	243.46	5	12	1071.01	966.88
8	C108-100	11	884.62	2	228.29	4	13	1112.92	1101.11
9	C109-100	10	911.29	2	187.07	6	12	1098.37	529.21
10	C201-100	4	683.10	1	61.06	1	5	744.16	1872.91
11	C202-100	4	677.48	1	47.98	2	5	725.46	760.49
12	C203-100	4	680.55	1	42.52	1	5	723.07	719.64
13	C204-100	4	690.80	1	61.06	1	5	751.85	1018.55
14	C205-100	4	676.29	1	61.06	1	5	737.35	1200.64
15	C206-100	4	772.26	0	0.00	0	4	772.26	1370.16
16	C207-100	4	679.16	1	70.75	3	5	749.92	647.67
17	C208-100	4	710.56	0	0.00	0	4	710.56	333.25
18	R101-100	23	1761.11	3	302.73	11	26	2063.84	3467.73
19	R102-100	20	1635.08	3	308.92	10	23	1944.01	3208.71
20	R103-100	16	1312.01	3	317.10	12	19	1629.12	1771.06
21	R104-100	15	1240.79	1	39.21	2	16	1280.00	2450.31
22	R105-100	19	1533.39	2	182.44	8	21	1715.84	1013.02
23	R106-100	17	1410.61	2	164.92	8	19	1575.53	1745.17
24	R107-100	15	1251.58	2	178.59	5	17	1430.17	1549.46
25	R108-100	12	1069.75	2	207.14	8	14	1276.89	1144.69
26	R109-100	16	1314.21	2	218.70	8	18	1532.90	1023.92
27	R110-100	14	1205.68	2	242.71	8	16	1448.40	844.78
28	R111-100	14	1233.64	3	217.46	10	17	1451.10	1620.80
29	R112-100	15	1230.13	1	78.01	2	16	1308.15	476.80
30	R201-100	6	1634.63	0	0.00	0	6	1634.63	408.99
31	R202-100	5	1069.86	0	0.00	0	5	1069.86	1197.89
32	R203-100	4	1093.77	0	0.00	0	4	1093.77	1338.03
33	R204-100	4	785.81	0	0.00	0	4	785.81	471.86

34	R205-100	5	1001.75	0	0.00	0	5	1001.75	1318.26
35	R206-100	4	940.36	0	0.00	0	4	940.36	246.21
36	R207-100	4	868.76	0	0.00	0	4	868.76	851.43
37	R208-100	3	773.04	0	0.00	0	3	773.04	270.93
38	R209-100	5	944.12	0	0.00	0	5	944.12	577.71
39	R210-100	4	1021.40	0	0.00	0	4	1021.40	783.70
40	R211-100	4	780.00	0	0.00	0	4	780.00	247.26
41	RC101-100	19	1806.84	2	279.27	7	21	2086.11	2196.60
42	RC102-100	17	1669.22	2	318.06	8	19	1987.29	3437.96
43	RC103-100	15	1512.94	1	139.86	4	16	1652.80	2225.84
44	RC104-100	13	1317.43	1	110.55	3	14	1427.97	1710.05
45	RC105-100	17	1650.40	3	317.25	10	20	1967.65	1342.06
46	RC106-100	16	1547.29	2	209.33	8	18	1756.62	1299.70
47	RC107-100	16	1488.77	1	156.80	4	17	1645.57	1558.41
48	RC108-100	14	1401.35	2	191.10	8	16	1592.45	2597.98
49	RC201-100	5	1482.87	0	0.00	0	5	1482.87	789.32
50	RC202-100	5	1207.72	0	0.00	0	5	1207.72	859.24
51	RC203-100	5	980.35	0	0.00	0	5	980.35	1351.08
52	RC204-100	4	827.14	0	0.00	0	4	827.14	1040.19
53	RC205-100	6	1275.21	0	0.00	0	6	1275.21	1006.38
54	RC206-100	5	1117.68	0	0.00	0	5	1117.68	958.29
55	RC207-100	5	1032.56	0	0.00	0	5	1032.56	496.38
56	RC208-100	4	832.92	0	0.00	0	4	832.92	1028.77

It can be observed in Table 8 that in different problem settings the use of BSVs and RSs are traded-off; there are cases where no BSVs are required (particularly instances of the second group with wider time windows such as C206-100, R201-100 and RC201-100) and there are cases where a few BSVs are well utilised to provide a large number of battery swaps (particularly instances of the first group with a random geographical distribution of customers such as R103-100 and R111-100). This implies that a logistics system based on the use of both RSs and BSVs presents flexibility and cost-saving opportunities and is well capable of accounting for the dynamics of the day-to-day freight distribution operations. We may also note that the relatively larger computational time of the MG-DP-ILNS compared with the DP-ILNS in Raeesi and Zografos (2020) is due to the recursive use of the multigraph-based DP for SCE within the MG-DP-ILNS which is more costly than the simple DP used for the EVRPTW-SMBS in DP-ILNS. However, given the extra complexity of the EVRPTW-RS-SMBS, the presented computational time can be considered quite reasonable and non-prohibitive.

For representation, and to see the combined use of intra-route recharging and on-the-fly battery swapping technologies in a solution to an EVRPTW-RS-SMBS, the ECV and BSV routes in the solution to one of the instances (i.e., C202-100) is presented in Figure 3.

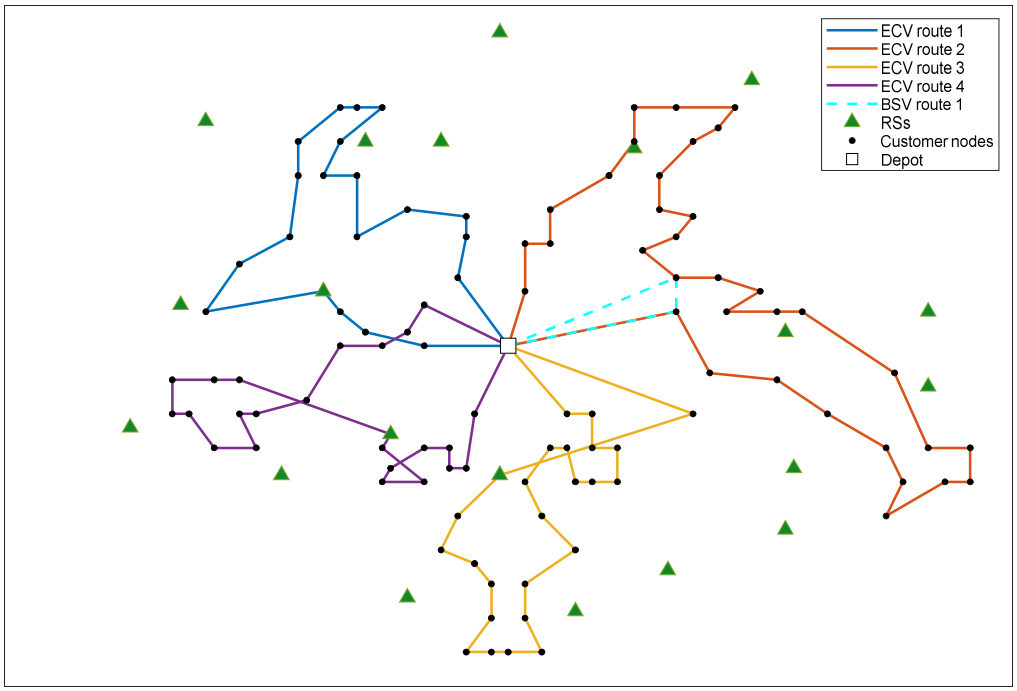

Figure 3 EVRPTW-RS-SMBS Solution to instance C202-100

In this figure, the EVRPTW-RS-SMBS solution yielded by the proposed MG-DP-ILNS algorithm requires 4 ECVs and 1 BSV. The ECVs travel a total distance of 677.48, visit 3 different RSs, and one of them (i.e., ECV route 2) requests a BSV to swap its battery twice over the course of its delivery route. The required BSV, on the other hand, travels a total distance of 47.98, yielding a total ECV and BSV travelled distance of 725.46. It is worth mentioning that the same instance under the setting of the EVRPTW-SMBS requires 5 vehicles in total (4 ECVs and 1 BSV) that travel a total distance of 803.85, and under the EVRPTW-RS setting requires 6 ECVs to travel a total distance of 1014.46.

6.5. The case study analysis: urban and regional scenarios

In section 5 of the paper, four different potential business scenarios were discussed for goods distribution via ECVs. In this section, we are using two realistic case studies generated in urban and regional levels to analyse the actual costs and emissions that result from each of these scenarios.

In the urban case (Figure 4.a. and Figure **5**.a.), we randomly generate the locations of a depot (containing a charging point) and 30 customers in Greater London (within a square grid of an approximate area of 2,116 km^2). Following this, the potential location of 7 other RSs with sufficient coverage of the area are manually selected. In the regional case (Figure 4.b. and Figure **5**.b.), the same set of nodes (i.e., a depot with a recharging point, 30 customers, and 7 RSs) are generated in Southeast England (within a square grid of an approximate area of 5,625 km^2).

a. b.

Figure 4 The areas of (a) the urban and (b) the regional cases

We assume a working day of 9 hours and attribute a random demand in the range [10kg,200kg] and a random time window with maximum width of 120 minutes to each customer. Service at all customer locations is also assumed to take 20 minutes. Pairwise distances between all nodes are calculated based on the ground driving distance returned by Bing Maps navigation, and thus the distance matrices in both cases are asymmetric (e.g., due to one-way roads). To calculate travel times, we have assumed an average

speed of 40 mph across both road networks. All data related to this case study are also available online in the link we referred to earlier.

a.

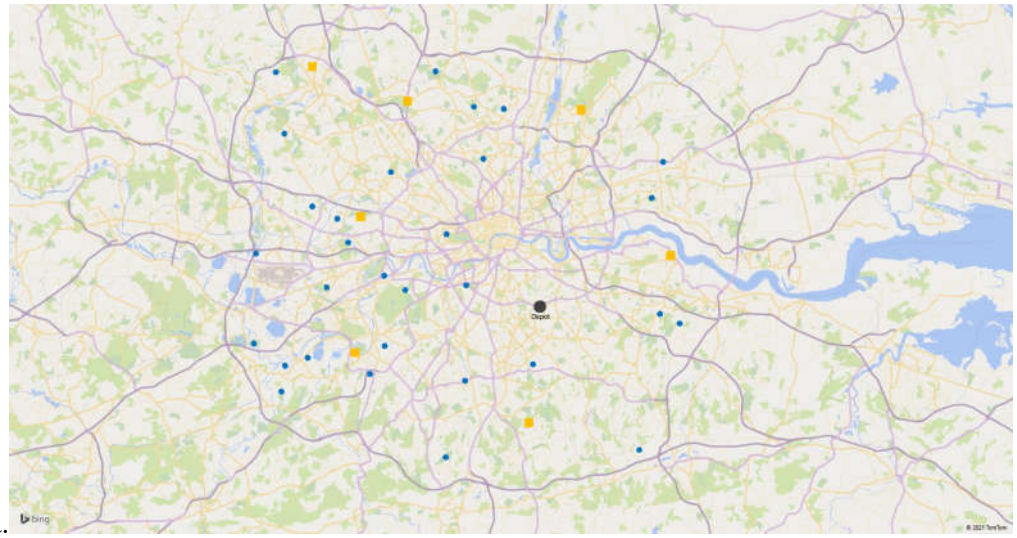

b.

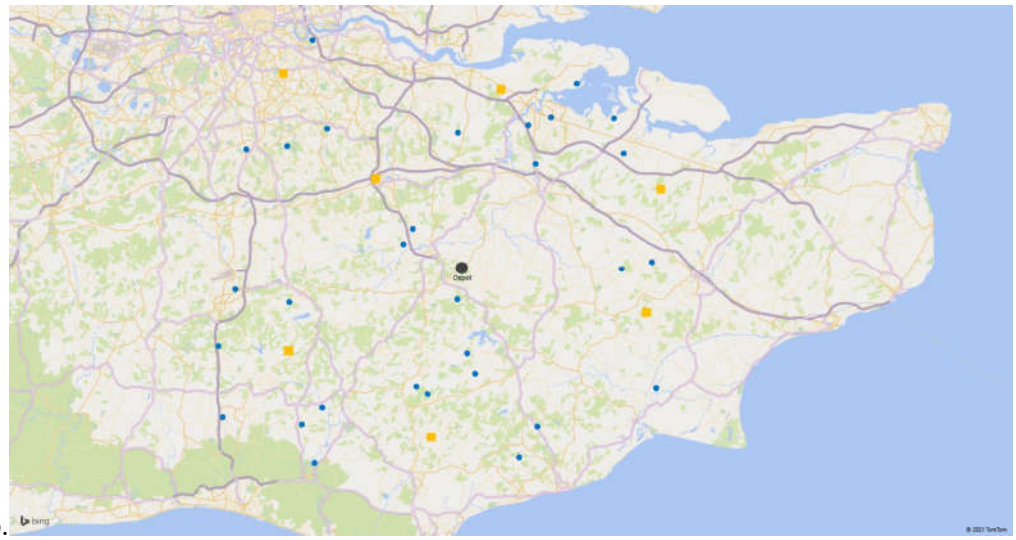

Figure 5 Locations of the depot, customers and RSs in (a) the urban and (b) the regional cases

The considered ECV included in the fleet is '*Renault Master Z.E.*', a full electric van with a 33-kWh lithium-ion battery. As of June 2021, Master Z.E.'s price is around £60,000 and the actual real-world driving range of the van reported by the company based on Worldwide Harmonized Light Vehicles Test Procedures (WLTP)[2] is 75 miles. It takes around 6 hours to fully recharge its battery at a fast 22kW recharging point, and the box van version has a maximum capacity of 1204 kg (20 m^3).

To calculate the TCO of the ECV and its daily cost (Ω_e), a lifetime of 10 years is considered, with 262 operational days in each year, and the purchase cost, battery cost and the release value at the end of the considered lifetime are included in the calculations. Given that Master Z.E. comes with a 5-year battery guarantee, we assume one battery pack replacement during the considered lifetime with the price of £4,785; calculated based on $200 per kWh price reported in Sanguesa et al. (2021). We also assume a release value of 20% of the original price at the end of the 10-year period. Operational costs ω_e, on the other hand, include the maintenance cost and fuel cost per km. For maintenance costs, we use £0.05/km based on the study of Lee et al. (2013) and fuel price is calculated at £0.08/km; giving a total of £0.13/km for ω_e.

For an eBSV, the same vehicle as the ECV can be assumed with additional purchasing and maintenance costs due to the swapping technology additions. Therefore, we assume BSVs are 40% more expensive than ECVs to purchase and maintain. It is assumed that they can carry 5 battery packs and given the on-board storage of battery packs have a driving range twice that of the ECV, and they can complete a battery swapping service in 10 minutes. As regards the iceBSVs, we assume the diesel equivalent of

[2] While actual real world driving results can defer due to factors such as weather conditions, driving styles and vehicle load, WLTP well represents everyday driving profiles and gives fuel consumption and driving range results that are much closer to real life conditions than other protocols as it is developed using real-driving data gathered from around the world.

the considered ECV/BSV, i.e., Renault Master, with its purchasing cost being around £29,000. Note that while the adoption cost of an ICEV is significantly less than that of an EV, ICEVs typically have a higher operational cost (Lee et al., 2013) as reflected in Table 9. Finally, we consider the well-to-wheel CO_2 emissions from an ECV or an eBSV (E_e) to be 55 g/km and that of an iceBSV (E_ι) to be 129 g/km based on the estimates from the JEC Consortium[3], which are close to lifecycle emission ratios between EVs and ICEVs reported in Lee et al. (2013).

The daily cost of an RS (Ω_r), on the other hand, is calculated based on land lease/purchase cost (£36,000), fast 22kw charger point cost (£1,550), maintenance cost per year (£250) and one-off labour instalment cost (£1,000) for the same 10-year lifetime, coming to a daily cost of £15.67 if opened. Note that, we assume the RS at the depot already exists, and the cost for other potential RSs is only incurred if they are opened and used in the routing plan.

Table 9 presents all values for the cost- and emissions-related parameters used within the scenarios. It is worth mentioning that to investigate the robustness of the proposed logistics model in this paper against cost assumptions made in Table 9, several sensitivity analyses are conducted and the summary of the results are reported in Appendix E. The results of the sensitivity analyses suggest that even under worst case scenarios the use of BSV's is beneficial both in terms of flexibility and business costs.

Table 9
Calculated values for cost and emissions related parameters

Cost/emission parameter	Value
Daily cost of an ECV (Ω_e)	£20.15
Daily cost of an eBSV (Ω_b)	£26.91
Daily cost of an iceBSV (Ω_b')	£12.40
Operational cost of an ECV per km (ω_e)	£0.13
Operational cost of an eBSV per km (ω_b)	£0.15
Operational cost of an iceBSV per km ($\omega_b{}'$)	£0.24
Daily cost of an RS (Ω_r)	£15.67
Daily cost of a lithium-ion battery pack (Ω_ι)	£3.65
WTW CO_2 emissions of ECVs/eBSVs in g/km (E_e)	55
WTW CO_2 emissions of iceBSVs in g/km (E_ι)	129

To perform the experiments, the path-based extension of the MILPs discussed for the scenarios in Section 5 are put into CPLEX, and without applying any restrictions on the solver, each problem is solved to optimality. Each MILP is solved using two different objective functions corresponding to: (i) the total cost, and (ii) the total amount of CO_2 emitted.

A visual comparison of the results obtained for the London and Southeast England cases is given in the radar charts in Figure 6. Note that there is no feasible route in the case of the Southeast England instance under Scenario I.

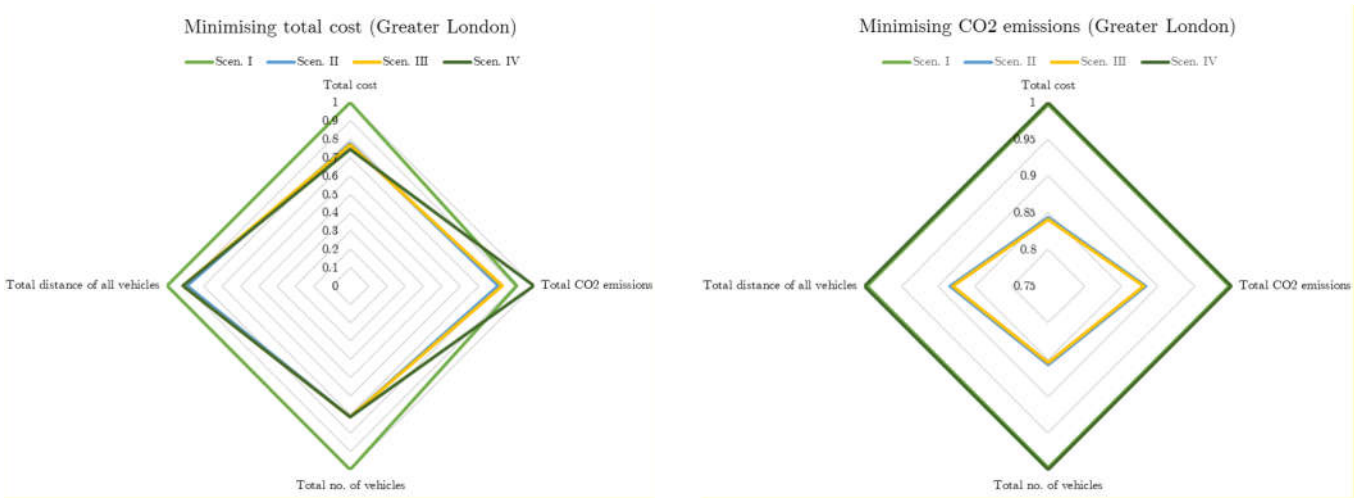

[3] https://gmobility.eu/what-is-well-to-wheel/

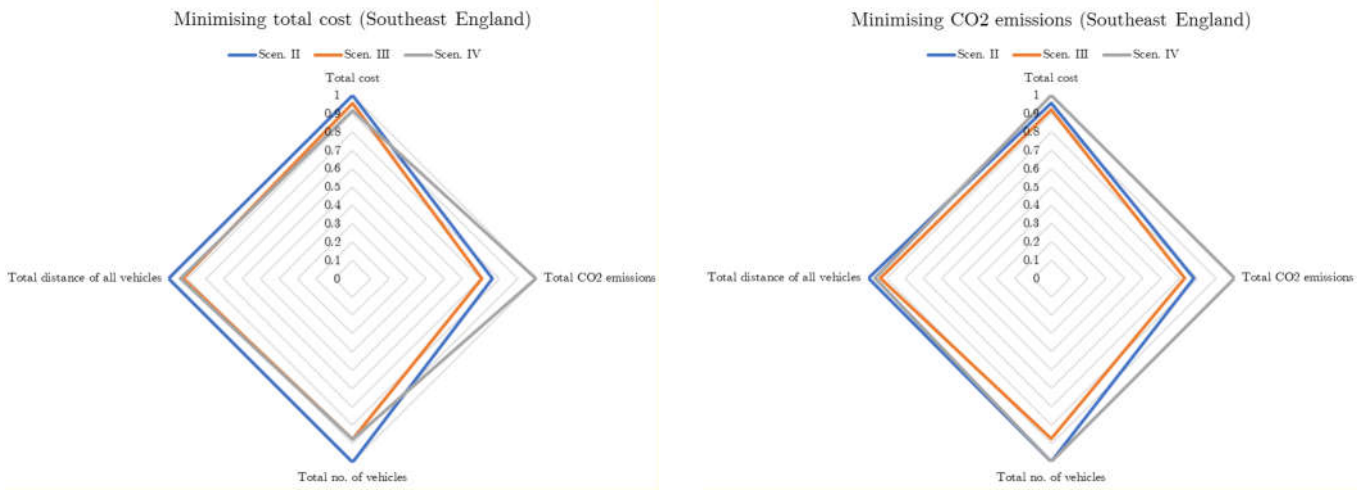

Figure 6 Comparison of results under each scenario in the urban and regional cases based on the business and environmental objectives

The detailed results of all these analyses are also presented in Table 10 and Table **11** for the urban and the regional cases, respectively. It is worth mentioning that values reported in the "minimisation of the business objective" case, are based on first minimising the business objective, and then minimising the environmental objective subject to the minimum cost found. Conversely, in the "minimisation of the environmental objective" case, we have first minimised the environmental objective, and then minimised the business objective subject to the minimum CO_2 emissions found.

Table 10
Comparison of scenarios in the urban case (Greater London)

	Minimising the business objective				Minimising the environmental objective			
	Scen. I	Scen. II	Scen. III	Scen. IV	Scen. I	Scen. II	Scen. III	Scen. IV
Total cost (£)	**257.67**	**200.63**	**198.19**	**192.05**	272.82	230.13	230.13	272.82
Total CO_2 emissions (kg)	36.08	32.12	32.94	39.83	**35.86**	**31.68**	**31.68**	**35.86**
Total no. of vehicles	7	5	5	5	7	6	6	7
Total distance of all vehicles (km)	656	584	599	599	652	576	576	652
Total no. of spare batteries	0	4	3	3	0	5	5	0
Total no. of opened RSs	3	0	1	1	4	0	0	4
No. of ECVs	7	4	4	4	7	4	4	7
No. of eBSVs	0	1	1	0	0	2	2	0
No. of iceBSVs	0	0	0	1	0	0	0	0
ECVs total distance (km)	656	454	506	506	652	447	447	652
eBSVs total distance (km)	0	130	93	0	0	129	129	0
iceBSVs total distance (km)	0	0	0	93	0	0	0	0

Table 10 shows that in the urban case when the business objective is considered, scenarios II, III and IV can respectively save around 22%, 23% and 25% in costs from the baseline scenario, i.e., scenario I. Note in the table that both scenarios II and III bring in cost savings simultaneous with savings in emissions (11% and 9%, respectively), but scenario IV reduces costs in scenario I by 25% at the cost of increasing emissions by around 10%.

For representation, the optimal routes under each scenario based on the business objective are illustrated in Figure 7. In this figure, the solid lines are the ECV routes, the dotted lines are the eBSV/iceBSV routes, and the triangles are RSs. Note that the routes yielded by scenarios III and IV are essentially the same, and the only reason for the reduced total cost in the case of scenario IV is the smaller purchasing cost of an iceBSV compared to that of an eBSV.

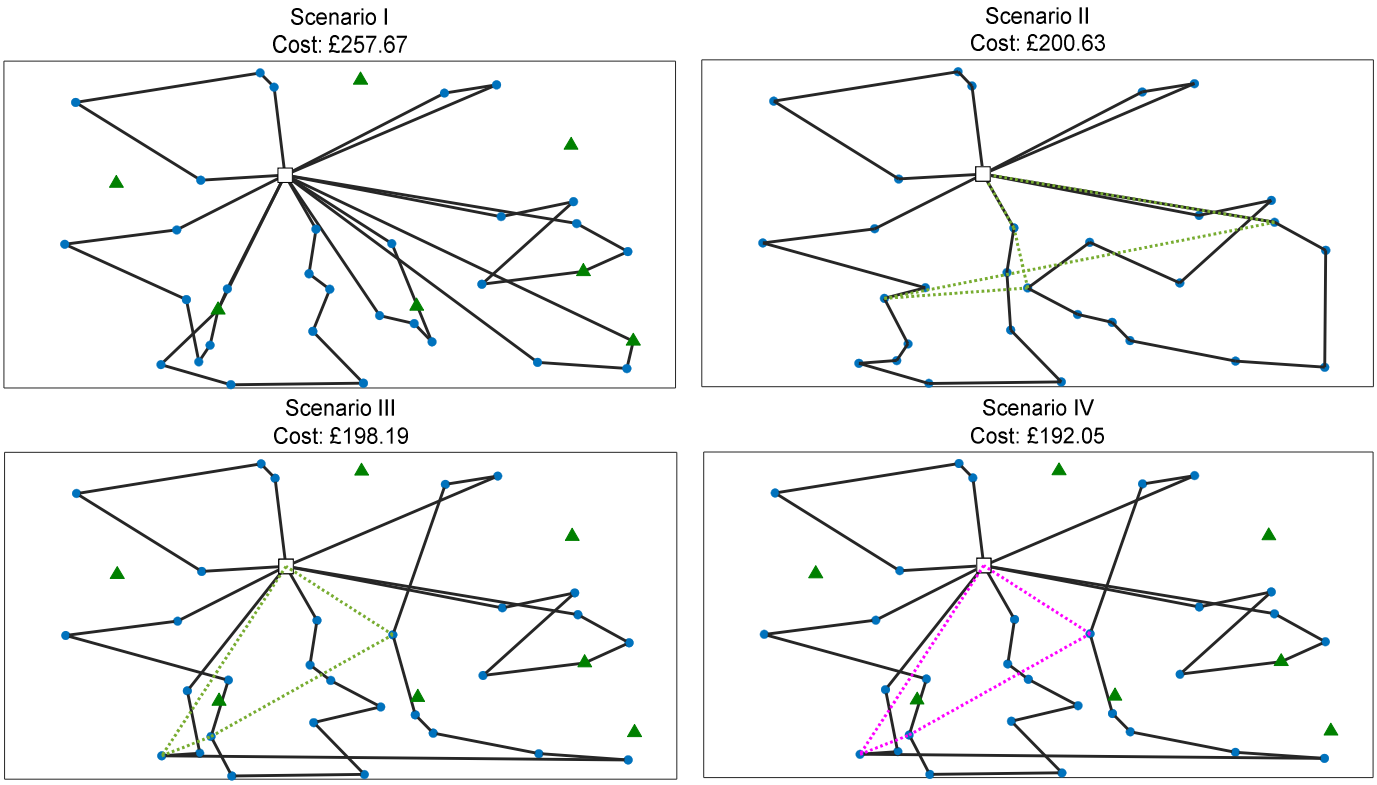

Figure 7 Optimal routes under each scenario in the urban case based on the business objective

When the CO_2 emissions minimisation objective function is considered for the optimisation models, on the other hand, scenario II (the mere use of eBSVs with no RSs) yields the best outcome. The table also shows that, even though the use of iceBSVs in scenario IV can significantly contribute to reducing the total number and distance of ECVs, they are not environmentally justifiable when the environmental objective is of prime importance and routing via visiting RSs is possible. All in all, in the urban case, scenario III provides the most promising performance when costs and emissions are considered together.

Table 11
Comparison of scenarios under the regional case (Southeast England)

	Minimising the business objective				Minimising the environmental objective			
	Scen. I	Scen. II	Scen. III	Scen. IV	Scen. I	Scen. II	Scen. III	Scen. IV
Total cost (£)	-*	**362.56**	**346.77**	**331.81**	-	363.81	349.89	379.73
Total emissions (kg)	-	60.94	56.32	79.83	-	**60.06**	**56.04**	**76.97**
Total no. of vehicles	-	8	7	7	-	8	7	8
Total distance of all vehicles (km)	-	1108	1024	1037	-	1092	1019	1051
Total no. of spare batteries	-	8	6	6	-	9	7	6
Total no. of opened RSs	-	0	2	1	-	0	2	3
No. of ECVs	-	5	5	5	-	5	5	6
No. of eBSVs	-	3	2	0	-	3	2	0
No. of iceBSVs	-	0	0	2	-	0	0	2
ECVs total distance (km)	-	716	732	729	-	716	721	792
eBSVs total distance (km)	-	392	292	0	-	376	298	0
iceBSVs total distance (km)	-	0	0	308	-	0	0	259

* Indicates that no feasible solution is found.

Table 11 presents results in the regional case where distances are larger and the limited driving range of ECVs is further prohibitive. Unsurprisingly, in such context there is no way to route ECVs with the mere option of diverting their routes to RSs and thus no feasible solution can be found under scenario I. On the other hand, the use of eBSVs and iceBSVs presents an interesting opportunity for supporting the routes of ECVs in performing extra-urban deliveries. Results in this table show again that scenario III provides an attractive mix in terms of costs and emissions, and while its cost is only marginally higher than scenario IV in the case of the business objective (only due to the much smaller purchase cost of an iceBSV compared with an eBSV), this scenario saves significantly in the total amount of CO_2 emitted. There may be cases of a wider geographical coverage where the driving

range of an eBSV is insufficient to cover the routes of the ECVs and that's when iceBSVs in conjunction with RSs can be quite helpful.

7. Discussion and conclusion

Widespread adoption of ECVs for goods distribution is a big step towards a zero-emissions road freight ecosystem. However, despite advances in emerging technologies pertaining to larger capacity electric batteries, rapid recharging points, and stationary/mobile battery swapping facilities, 'range anxiety' is still a pervasive barrier in the face of logistics adoption of ECVs. To increase the driving range of running ECVs for completing their delivery tasks, the electric vehicle routing research has thus far mainly focused on ways to facilitate intra-route recharging via pre-planned diverted visits to privately owned RSs. Newer research has also proposed the use of BSVs and the synchronised mobile battery swapping option as an alternative way of overcoming the issue of 'range anxiety' in ECVs. This paper focused on a variant of the EVRPTW, referred to as the EVRPTW-RS-SMBS, in which visits to available RSs and requests for the mobile battery swapping service are simultaneously considered. In the proposed problem ECVs are permitted to increase their driving range by either visiting a nearby RS or calling a BSV for performing a battery swapping service at a coordinated rendezvous time and space. Routing is carried out in two interdependent levels for the ECVs and the BSVs, and in one level (i.e., ECVs level) potential visits to RSs are also considered.

While the EVRPTW-RS-SMBS promises a guaranteed performance over both the EVRPTW-RS and the EVRPTW-SMBS due to its extended solution space, combining the required spatiotemporal synchronisation between the routes of ECVs and BSVs with the possible intra-route visits to RSs brings in significant methodological complications that hinder its pragmatic implementation and deployment. To tackle these complications and solve practical instances of the problem within a reasonable computational time, the paper proposed several combinatorial results for deriving a path-based MILP formulation and a path-based DP used within a heuristic solution algorithm.

In order to establish a case for the proposed logistics model and to shed light on the influence of the various strategic/tactical and operational costs that incur for simultaneously providing two alternative systems for extending the driving range of the ECVs (e.g., cost of RSs, BSVs, and extra spare battery packs needed), the paper considered four alternative business scenarios for operating on ECVs and performed various comparative analyses (cost and emissions) using realistic case studies generated in urban and regional levels in the UK. These case studies along with other test instances put forth by the paper provided several insights on the added value of the proposed problem variant and the developed exact and heuristic solution algorithms. Our results on instances with 100 customers and 21 RSs indicate that the total number of vehicles needed (ECVs and BSVs) in an EVRPTW-RS-SMBS solution can be up to 33% less than that of an EVRPTW-SMBS solution (8% on average over all instances), and up to 41% less than the number of ECVs required in an EVRPTW-RS solution (14% on average over all instances). When the number of vehicles required in the case of the solution from the EVRPTW-RS-SMBS is equal to those of the EVRPTW-SMBS and the EVRPTW-RS, the EVRPTW-RS-SMBS solution saves significantly in the total distance travelled (up to 52% in the case of the EVRPTW-SMBS and up to 13% in the case of the EVRPTW-RS). We further showed that by just putting a path-based formulation of the EVRPTW-RS-SMBS and its related problem class, i.e., EVRPTW-RS into a commercial solver several difficult instances that are otherwise intractable for regular MILP formulations based on the use of dummy copies of RSs could be solved to optimality. Our computational results also demonstrated the favourable performance of the proposed MG-DP-ILNS algorithm in solving larger instances of the EVRPTW-RS-SMBS. Finally, results from the comparative analysis of the business scenarios using the urban and regional case studies indicated that a logistics design based on the simultaneous use of BSVs and RSs not only can save greatly in costs and CO_2 emissions, but also this can open up new opportunities for inter-urban deliveries using ECVs. The proposed model fits also very well with the real nature of the small package delivery sector in which customers locations change on a daily basis. With BSVs, a much greater level of flexibility is brought in as routes are not merely tied to the fixed location of established RSs or battery swapping stations.

There are multiple further research opportunities in the area of EVRPTWs with various technological options. An integrated location-routing framework where multiple technologies such as rapid recharging points, Battery Recharging Vans (BRVs), stationary and mobile battery swapping are considered simultaneously would be an important contribution to designing a logistics network based on the use of ECVs. In the scenarios considered in this paper, we assumed the company owns the BSV fleet. With further development and deployment of these technologies, however, new business models can emerge for providing non-stationary battery swapping/recharging, and logistics companies may decide to subscribe to these companies for the required service instead of including BSVs in their fleet and managing them themselves. The benefits of outsourcing such service to a third-party provider, however, is subject to further research as it depends on many factors such as the trade-off with the subscription price charged by the service provider which is in turn dependant on the scale of their demand and the maturity of the technology. Along the same lines,

another important direction for future research would be to develop logistics models tailored for BSV/BRV providers who serve multiple freight distribution companies running on ECVs. Corresponding solutions for BSV/BRV providers would need to entail provision and distribution models incorporating decisions regarding the storage and maintenance of an inventory of spare electric batteries simultaneous with routing, scheduling and synchronisation decisions. An important element of the proposed logistics technique in this paper pertains to the use of BSVs for carrying lithium-ion battery packs to the point where they are needed. At the same time, lithium-ion batteries are hazardous goods and their transportation is a highly regulated with specific procedures and guidelines (e.g., temperature control, stability, and exposure to conductive surfaces). Therefore, future research can extend the proposed model in this paper by treating the routing at the BSV tier with features from the vehicle routing for hazardous materials transportation literature. Future research can also extend the proposed model in this paper to incorporate more realistic assumptions in terms of the energy consumption of ECVs and BSVs, the battery recharging functions, the battery recharging levels, and the travel and service/recharging times using more detailed nonlinear energy consumption models and the use of stochastic/robust optimisation to handle the related uncertainties and dynamics. Finally, we argue that there is a lot of potential for further algorithmic developments in tackling the proposed problem in this paper as there are multiple complications that are specific to the proposed problem variant which may also contribute to our understanding of other related routing problems such as the truck-drone routing problem.

Appendices

Appendix A. List of the notation and acronyms

The following table presents the key notation used in the text. We have attempted to keep unique meaning for each notation to the greatest extent possible. In those cases where an item has additional uses, they should be clear from context.

Notation	Definition
G	A complete directed graph
$\boldsymbol{V}$	The vertex set in G
$\boldsymbol{A}$	The set of directed arcs in G
$\boldsymbol{N}$	The set of customer nodes in V
$\boldsymbol{R}$	The set of RSs
$\boldsymbol{n}$	Number of customers
$\boldsymbol{r}$	Number of RSs
$\boldsymbol{q_i}$	Demand requested by customer $i \in N$
$\boldsymbol{e_i}$	Lower boundary of the time window of customer $i \in N$
$\boldsymbol{l_i}$	Upper boundary of the time window of customer $i \in N$
$\boldsymbol{s_i}$	Service time at customer $i \in N$
$\boldsymbol{d_{ij}}$	Distance of arc $(i,j) \in A$
$\boldsymbol{t_{ij}}$	Travel time of arc $(i,j) \in A$
$\boldsymbol{Q_e}$	Maximum payload of each ECV
$\boldsymbol{C_e}$	Battery capacity of each ECV
$\boldsymbol{r_e}$	Energy consumption rate of each ECV
$\boldsymbol{Q_b}$	Maximum number of batteries each BSV can carry
$\boldsymbol{C_b}$	Battery capacity of each BSV
$\boldsymbol{r_b}$	Energy consumption rate of each BSV
$\boldsymbol{g}$	ECV's recharging rate at an RS
$\boldsymbol{\lambda}$	Swapping service time
$\boldsymbol{\sigma}$	Dummy copy of the depot $\{0\}$ referred to as the final depot
$\boldsymbol{R'}$	An extended RSs set with dummy nodes to allow multiple visits to each RS
$\boldsymbol{V'}$	$N \cup R'$
$\boldsymbol{V_0}$	$\{0\} \cup N$
$\boldsymbol{V_\sigma}$	$N \cup \{\sigma\}$
$\boldsymbol{V'_0}$	$\{0\} \cup N \cup R'$
$\boldsymbol{V'_\sigma}$	$N \cup R' \cup \{\sigma\}$
$\boldsymbol{\mathcal{A}}$	The set of directed arcs between all nodes in G, except those in R'
$\boldsymbol{x_{ij}}$	Binary decision variable indicating if arc $(i,j) \in A$ is traversed by an ECV
$\boldsymbol{z_{ij}}$	Binary decision variable indicating if arc $(i,j) \in \mathcal{A}$ is traversed by a BSV
$\boldsymbol{y_i}$	Decision variable denoting the time of arrival of an ECV at node $i \in V$
$\boldsymbol{w_i}$	Decision variable denoting the time of arrival of a BSV at node $i \in V \backslash R'$
$\boldsymbol{f_i}$	Decision variable specifying the remaining load on an ECV upon arrival at node $i \in V$
$\boldsymbol{h_i}$	Decision variable specifying the number of the remaining fully-charged batteries on the BSV upon arrival at node $i \in V \backslash R'$
$\boldsymbol{u_i}$	Decision variable indicating the remaining battery charge level of an ECV on arrival at node $i \in V$; also denoting the BCL in section 4.1.

$\boldsymbol{v_i}$	Decision variable indicating the remaining battery charge level of a BSV on arrival at node $i \in V \backslash R'$
$\boldsymbol{V_r}$	Required nodes; i.e., nodes on G that represent the location of the depot and the customers
$\boldsymbol{\epsilon_{ij}}$	Direct edge; simply an arc $(i,j) \in A | i,j \in V_r, i \neq j$
$\boldsymbol{p_{ij}}$	An RS-path connecting a pair of required nodes $i,j \in V_r$
$\boldsymbol{\mathcal{p}_{ij}}$	The set of all possible RS-paths between a pair of required nodes $i,j \in V_r$
$\boldsymbol{d(p_{ij,\mathcal{J}})}$	Distance of an RS-path $p_{ij,\mathcal{J}} \in \mathcal{p}_{ij}$
$\boldsymbol{\tau^{u_i}(p_{ij,\mathcal{J}})}$	Travel time of an RS-path $p_{ij,\mathcal{J}} \in \mathcal{p}_{ij}$ when the origin is left at u_i BCL
$\boldsymbol{\mathbb{t}_{ij,\mathcal{J}}}$	Travel time of $p_{ij,\mathcal{J}} \in \mathcal{p}_{ij}$ when $u_i = C_e$
$\boldsymbol{\pi(p_{ij,\mathcal{J}})}$	The discharged level of the ECV's battery upon arrival at the endpoint of the RS-path $p_{ij,\mathcal{J}} \in \mathcal{p}_{ij}$
$\boldsymbol{\varphi(p_{ij,\mathcal{J}})}$	MR-BCL attribute of RS-path $p_{ij,\mathcal{J}} \in \mathcal{p}_{ij}$
$\boldsymbol{E(p_{ij,\mathcal{J}})}$	4D eligibility vector of RS-path $p_{ij,\mathcal{J}} \in \mathcal{p}_{ij}$
$\boldsymbol{\mathfrak{p}_{ij}}$	Set of all eligible paths between a pair of required nodes $i,j \in V_r$
$\boldsymbol{\mathcal{G}}$	Multigraph constructed from required nodes only and the direct edges and eligible paths between them.
$\boldsymbol{\mathcal{P}_{ij}}$	Superset of ϵ_{ij} and $\mathfrak{p}_{ij}$ between a pair of required nodes $i,j \in V_r$
$\boldsymbol{\mathcal{P}}$	Set of all $\mathcal{P}_{ij}$s for all pairs of required nodes $i,j \in V_r$ (arcs in $\mathcal{G}$)
$\boldsymbol{\mathcal{E}(p_{ij,\mathcal{J}})}$	3D eligibility vector of RS-path $p_{ij,\mathcal{J}} \in \mathcal{p}_{ij}$
$\boldsymbol{\overline{v}}$	The average speed in the network
$\boldsymbol{\alpha_{ijp}}$	Precomputed modelling parameter for each path $(i,j,p) \in \mathcal{P}_{ij}$ used in the path-based formulation
$\boldsymbol{\beta_{ijp}}$	Precomputed modelling parameter for each path $(i,j,p) \in \mathcal{P}_{ij}$ used in the path-based formulation
$\boldsymbol{\gamma_{ijp}}$	Precomputed modelling parameter for each path $(i,j,p) \in \mathcal{P}_{ij}$ used in the path-based formulation
$\boldsymbol{\delta_{ijp}}$	Precomputed modelling parameter for each path $(i,j,p) \in \mathcal{P}_{ij}$ used in the path-based formulation
$\boldsymbol{x_{ijp}}$	Binary decision variable indicating if path $(i,j,p) \in \mathcal{P}$, is traversed by an ECV
$\boldsymbol{z_{ij1}}$	Binary decision variable indicating if path $(i,j,1) \in \mathcal{P}$ is traversed by a BSV
$\boldsymbol{\Omega_e}$	The daily cost of an ECV
$\boldsymbol{\Omega_r}$	The daily cost of an opened RS
$\boldsymbol{\Omega_b}$	The daily cost of an eBSV
$\boldsymbol{\Omega_l}$	The daily cost of each spare lithium-ion battery pack
$\boldsymbol{\Omega_b{}'}$	The daily cost of an iceBSV
$\boldsymbol{\omega_e}$	The operational cost of each km travelled by an adopted ECV
$\boldsymbol{\omega_b}$	The operational cost of each km travelled by an adopted eBSV
$\boldsymbol{\omega_b{}'}$	The operational cost of each km travelled by an adopted iceBSV
$\boldsymbol{E_e}$	kg/km CO_2 emitted by an ECV/eBSV
$\boldsymbol{E_\iota}$	kg/km CO_2 emitted by an iceBSV
$\boldsymbol{O_i}$	Binary variable denoting whether RS $i \in R$ is opened or not
$\boldsymbol{\Pi_{pi}}$	Binary input parameters indicating whether path $p \in \mathcal{P}$ passes through RS $i \in R$

The following table presents the list of acronyms used within the paper:

Acronym	Meaning
BaaS	Battery as a Service
BCL	Battery Charge Level
BRV	Battery Recharging Van
BSV	Battery Swapping Van
CaaS	Charging-as-a-Service
CGG	Charge Gained and Gone
DP-ILNS	Dynamic Programming based Intensified Large Neighbourhood Search
DPIP	Dynamic Programming and an Integer Programming
EBDL	Endpoint Battery Discharge Level
eBSV	electric BSV
ECV	Electric Commercial Vehicle
EVRPTW-RS	Electric Vehicle Routing Problem with Time Windows and Recharging Stations
EVRPTW-SMBS	Electric Vehicle Routing Problem with Time Windows and Synchronised Mobile Battery Swapping
EVRPTW-RS-SMBS	Electric Vehicle Routing Problem with Time Windows, Recharging Stations and Synchronised Mobile Battery Swapping
FSASP	Fixed Sequence Arc Selection Problem
iceBSV	internal combustion engine BSV
ICEV	Internal Combustion Engine Vehicle
MILP	Mixed Integer Linear Programming
MG-DP	Multi-Graph based Dynamic Programming
MR-BCL	Minimum Required BCL
NDPI	Non-Dominated Path Identification
RS	Recharging Station
SCE	Solution Cost Evaluation
SoC	State of Charge
TCO	Total Cost of Ownership

Appendix B. Extension of Observation 1 to the case of a nonlinear charging function

Montoya et al. (2017) show that a piecewise linear concave charging function like the one shown in Figure B.1 can provide a close approximation for the actual nonlinear charging function at a given RS. As illustrated in the figure, we denote by the set $B = \{0, \dots, b\}$ the ordered set of breakpoints in the given piecewise linear charging function. Also, we denote by τ_k and ρ_k the charging time and the BCL of breakpoint $k \in B$ (so that $\rho_b = C_e$, and τ_b is the total time required to fully charge an ECV battery at the given RS from zero BCL). The line segment connecting ρ_k to ρ_{k+1} has a slope μ_k equal to $(\rho_{k+1} - \rho_k)/(\tau_{k+1} - \tau_k)$, and an intercept ϕ_k equal to $(\rho_k - \mu_k \tau_k), \forall k \in \{0, \dots, b-1\}$. Given that an ECV arrives at the RS $i \in R$ with BCL $u_i \in [\rho_k, \rho_{k+1}), k \in \{0, \dots, b-1\}$, the time taken for fully recharging the ECV's battery at the RS would be equal to $\tau_b - [(u_i - \phi_k)/\mu_k]$.

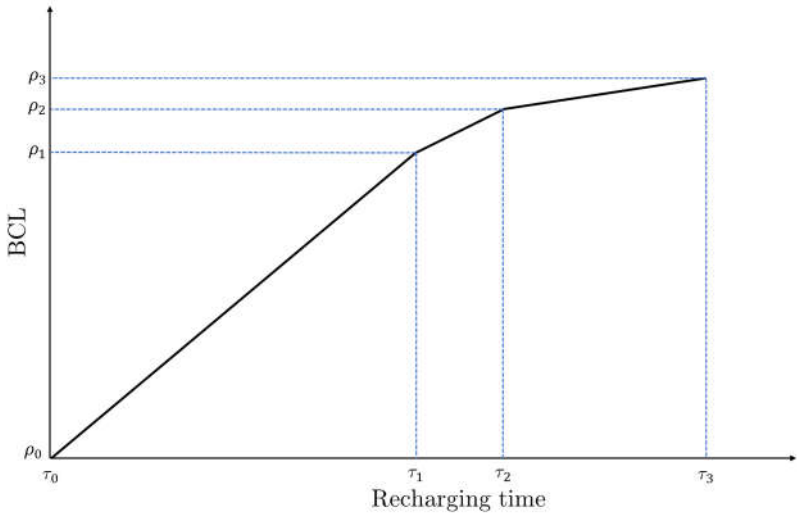

Figure B.1. A piecewise linear charging function

To extend Observation 1 to the case of a nonlinear recharging function, consider the RS-path $p_{ij,\mathcal{J}} = [(i,1),(1,2),\dots,(n,j)], 1..n \in R$ which connects a pair of required nodes $i, j \in V_r, i \neq j$. Let $\Gamma_{ij,\mathcal{J}}$ be the travel time of the segment $[(1,2),\dots,(n,j)]$ of $p_{ij,\mathcal{J}}$ (i.e., after the first RS, i.e., RS 1, in the path). Note that upon leaving RS 1 the ECV is fully charged and it is therefore possible to pre-compute $\Gamma_{ij,\mathcal{J}}$. Then, Observation 1 can be extended to Observation B.1. for the case of a piecewise linear concave charging function for the RSs as follows:

Observation B.1 *Regardless of the number of RSs visited on the RS-path $p_{ij,\mathcal{J}} \in \mathcal{P}_{ij}$, knowing u_i is necessary and sufficient to compute $\tau^{u_i}(p_{ij,\mathcal{J}})$ using the closed form expression $\tau^{u_i}(p_{ij,\mathcal{J}}) = \Gamma_{ij,\mathcal{J}} + t_{i1} + \tau_b - [(u_i - \varphi(p_{ij,\mathcal{J}}) - \phi_k)/\mu_k]$, where $[u_i - \varphi(p_{ij,\mathcal{J}})] \in [\rho_k, \rho_{k+1}), k \in \{0, \dots, b-1\}$ (refer to Definition 3 in the paper for the definition of $\varphi(p_{ij,\mathcal{J}})$).*

Appendix C. Proofs of lemmas and the theorem

C.1. Proof of Lemma 1

Proof. The condition that $\tau^{C_e}(p_{ij,1}) \leq \tau^{C_e}(p_{ij,2})$ means that the travel time of $p_{ij,1}$ when $u_i = C_e$, i.e., $\mathbb{t}_{ij,1}$, is less than or equal to the travel time of $p_{ij,2}$ when $u_i = C_e$, i.e., $\mathbb{t}_{ij,2}$. Hence, for any given $u_i \in [\varphi(p_{ij,1}), C_e]$, we have $\mathbb{t}_{ij,1} + g(C_e - u_i) \leq \mathbb{t}_{ij,2} + g(C_e - u_i)$, and thus, $\tau^{u_i}(p_{ij,1}) \leq \tau^{u_i}(p_{ij,2})$. □

C.2. Proof of Theorem 1

Proof. Suppose $\mathcal{S} = \mathcal{R}_1, \mathcal{R}_2, \dots, \mathcal{R}_k$ indicates an optimal solution to an instance of the EVRPTW-RS-SMBS that is solved on G, where each $\mathcal{R}_\mathscr{k}, \forall \mathscr{k} \in \{1, .., k\}$ denotes an ECV route in $\mathcal{S}$. Each route $\mathcal{R}_\mathscr{k} \in \mathcal{S}$ could be viewed as a path that starts at the depot 0, visits a set of customers $N_\mathscr{k} \subseteq N$ (and possibly some intermediate RSs), and terminates at the depot σ. Since $\mathcal{S}$ is an optimal solution to the problem, each route $\mathcal{R}_\mathscr{k} \in \mathcal{S}$ is resource feasible and has a smaller total distance than any other path visiting the same sequence of customers in $N_\mathscr{k}$. Hence, we must prove that the elimination of redundant paths between each pair of required nodes i and j in $\mathcal{R}_\mathscr{k}$ has no implications regarding the resource-feasibility and optimality of $\mathcal{R}_\mathscr{k}$. To do so, suppose that a set of labels are maintained at each required node along $\mathcal{R}_\mathscr{k}$, each one corresponding to a partial path issued from 0 and containing the cumulative consumption level of each resource at the end of the corresponding partial path. The three resources we need to keep track of are distance, time

and the BCL, with the latter two being constrained. Note that vehicle capacity is irrelevant as $\mathcal{R}_\ell$ is already capacity feasible and elimination of RS-paths has no effect on its capacity feasibility. For both of the constrained resources time and BCL, at each required node g in $\mathcal{R}_\ell$, resource windows could be defined, where for the time resource, we have customers' time-windows $[e_g, l_g]$, and for the BCL resource we have BCL-windows $\left[\min_{p_{gh,\mathcal{J}} \in \mathcal{P}_{gh}} \varphi(p_{gh,\mathcal{J}}), C_e\right]$. Note that the RS-path with $\min_{p_{gh,\mathcal{J}} \in \mathcal{P}_{gh}} \varphi(p_{gh,\mathcal{J}})$ already exists in $\mathfrak{p}_{gh}$, and elimination of redundant paths has had no effect on the resource windows. Hence, let the label $L_g = [\mathbb{I}_g^{dist}, \mathbb{I}_g^{time}, u_g]$ denote the consumption level of distance, time, and the BCL up to the required node g in $\mathcal{R}_\ell$, respectively. Note that the larger values of u_g are desirable. The initial label is $L_0 = [0, e_0, C_e]$, and the extension of a label along an RS-path $p_{gh,\mathcal{J}} \in \mathcal{P}_{gh}$ from g to h in $\mathcal{R}_\ell$ is performed using the following Resource Extension Functions (REF) (note that we just need to focus on RS-paths rather than direct edges as they are already present in both $\mathcal{G}$ and G):

$$\mathbb{I}_h^{dist} = \mathbb{I}_g^{dist} + d(p_{gh,\mathcal{J}}) \tag{41}$$

$$\mathbb{I}_h^{time} = \mathbb{I}_g^{time} + \mathbb{t}_{gh,\mathcal{J}} + g(C_e - u_g) \tag{42}$$

$$u_h = C_e - r_e d_{nh} \tag{43}$$

Using these REFs we can prove that the labels extended by any redundant path along $\mathcal{R}_\ell$ are always dominated by the labels extended using eligible paths. To do so, assume $p_{gh,1}$ is an eligible path that is present in $\mathcal{G}$, whereas $p_{gh,2}$ is a redundant path discarded from $\mathcal{G}$. Since the eligibility of $p_{gh,1}$ and the redundancy of $p_{gh,2}$ implies that $E(p_{gh,1}) \preccurlyeq E(p_{gh,2})$ (Definition 5), it is easy to see that for any given $\mathbb{I}_g^{dist}$, we always have $\mathbb{I}_g^{dist} + d(p_{gh,1}) \leq \mathbb{I}_g^{dist} + d(p_{gh,2})$, and also we always have $C_e - r_e d_{\ell h,1} \geq C_e - r_e d_{\ell h,,2}$. Moreover, based on Lemma 1, as long as $u_g \geq \varphi(p_{gh,1})$, the fact that $\tau^{C_e}(p_{gh,1}) \leq \tau^{C_e}(p_{gh,2})$ (Definition 5), implies that $\mathbb{t}_{gh,1} + g(C_e - u_g) \leq \mathbb{t}_{gh,2} + g(C_e - u_g)$, and hence $\mathbb{I}_g^{time} + \mathbb{t}_{gh,1} + g(C_e - u_g) \leq \mathbb{I}_g^{time} + \mathbb{t}_{gh,1} + g(C_e - u_g)$. On the other hand, for values of $u_g < \varphi(p_{gh,1})$ when path $p_{gh,1}$ is infeasible, path $p_{gh,2}$ is also definitely infeasible as $E(p_{gh,1}) \preccurlyeq E(p_{gh,2})$ implies $\varphi(p_{gh,1}) \leq \varphi(p_{gh,2})$. □

C.3. Proof of Lemma 2

Proof. To prove the lemma, we need to show that if $\mathcal{E}(p_{ij,1}) \preccurlyeq \mathcal{E}(p_{ij,2})$, then $d(p_{ij,1}) \leq d(p_{ij,2})$. Suppose $p_{ij,1} = [(i, v_{11}), \dots, (v_{n1}, j)], v_{11} .. v_{n1} \in R$, and $p_{ij,2} = [(i, v_{12}), \dots, (v_{n2}, j)], v_{12} .. v_{n2} \in R$. We may write the distance and the travel time (at full BCL) of each of these RS-paths as: $d(p_{ij,\mathcal{J}}) = d_{iv_{1\mathcal{J}}} + d_{v_{1\mathcal{J}} \dots v_{n\mathcal{J}}} + d_{v_{n\mathcal{J}} j}$ and $\tau^{C_e}(p_{ij,\mathcal{J}}) = t_{iv_{1\mathcal{J}}} + t_{v_{1\mathcal{J}} \dots v_{n\mathcal{J}}} + t_{v_{n\mathcal{J}} j} + gr_e(d_{iv_{1\mathcal{J}}} + d_{v_{1\mathcal{J}} \dots v_{n\mathcal{J}}}), \forall \mathcal{J} \in \{1,2\}$, respectively, where $d_{v_{1\mathcal{J}} \dots v_{n\mathcal{J}}}$ and $t_{v_{1\mathcal{J}} \dots v_{n\mathcal{J}}}$ denote the total distance and travel time of the arcs between the first and the last RS on $p_{ij,\mathcal{J}}$. If there is only one RS on $p_{ij,\mathcal{J}}$, then both $d_{v_{1\mathcal{J}} \dots v_{n\mathcal{J}}}$ and $t_{v_{1\mathcal{J}} \dots v_{n\mathcal{J}}}$ are 0. Now, to prove the lemma, we use a proof by contradiction, where we assume despite $\mathcal{E}(p_{ij,1}) \preccurlyeq \mathcal{E}(p_{ij,2})$, we have (44) below:

$$d(p_{ij,1}) > d(p_{ij,2}) \tag{44}$$

The condition that $\mathcal{E}(p_{ij,1}) \preccurlyeq \mathcal{E}(p_{ij,2})$, yields:

$$t_{iv_{11}} + t_{v_{11} \dots v_{n1}} + t_{v_{n1} j} + gr_e(d_{iv_{11}} + d_{v_{11} \dots v_{n1}}) \leq t_{iv_{12}} + t_{v_{12} \dots v_{n2}} + t_{v_{n2} j} + gr_e(d_{iv_{12}} + d_{v_{12} \dots v_{n2}}) \tag{45}$$

On the other hand, based on the linear dependency assumption between travel time and distance, following (44) we have:

$$t_{iv_{11}} + t_{v_{11} \dots v_{n1}} + t_{v_{n1} j} > t_{iv_{12}} + t_{v_{12} \dots v_{n2}} + t_{v_{n2} j} \tag{46}$$

Considering (45) and (46), for (45) to hold true, we must have:

$$gr_e(d_{iv_{11}} + d_{v_{11} \dots v_{n1}}) \leq gr_e(d_{iv_{12}} + d_{v_{12} \dots v_{n2}}) \tag{47}$$

Which means:

$$d_{iv_{11}} + d_{v_{11} \dots v_{n1}} \leq d_{iv_{12}} + d_{v_{12} \dots v_{n2}} \tag{48}$$

At the same time, as another implication of $\mathcal{E}(p_{ij,1}) \preccurlyeq \mathcal{E}(p_{ij,2})$, we know $\varphi(p_{ij,1}) \leq \varphi(p_{ij,2})$, which means $r_e d_{v_{n1} j} \leq r_e d_{v_{n2} j}$, and hence:

$$d_{v_{n1} j} \leq d_{v_{n2} j} \tag{49}$$

The combination of (48) and (49) results in $d(p_{ij,1}) \leq d(p_{ij,2})$, which is in contradiction with (44). □

Appendix D. The complete path-based formulation for the EVRPTW-RS-SMBS

The path-based MILP for the EVRPTW-RS-SMBS is given below:

$$z_1 := \sum_{(0,j,p)\in\mathcal{P}} x_{0jp} + \sum_{(0,j,1)\in\mathcal{P}} z_{0jp} \tag{50}$$

$$z_2 := \sum_{(i,j,p)\in\mathcal{P}} d_{ijp}x_{ijp} + \sum_{(i,j,1)\in\mathcal{P}} d_{ij1}z_{ij1} \tag{51}$$

$$lex\min(z_1, z_2) \tag{52}$$

Subject to:

$$\sum_{j\in V_\sigma}\sum_{p\in\mathcal{P}_{ij}} x_{ijp} = 1, \qquad \forall i \in N \tag{53}$$

$$\sum_{j\in V_0}\sum_{p\in\mathcal{P}_{ji}} x_{jip} - \sum_{j\in V_\sigma}\sum_{p\in\mathcal{P}_{ij}} x_{ijp} = 0, \qquad \forall i \in N \tag{54}$$

$$\sum_{j\in V_0} z_{ji1} - \sum_{j\in V_\sigma} z_{ij1} = 0, \qquad \forall i \in N \tag{55}$$

$$y_i + \alpha_{ijp}u_i + (\beta_{ijp} + s_i)x_{ijp} + \lambda \sum_{\vartheta\in V_0: i\neq 0} z_{\vartheta i1} - (l_0 + \lambda)(1 - x_{ijp}) \le y_j, \qquad \forall (i,j,p)\in\mathcal{P} | i\in V_0, j\in V_\sigma, i\neq j \tag{56}$$

$$w_i \le y_i + s_i, \qquad \forall i \in V \tag{57}$$

$$y_i + \alpha_{ij1}v_i + (\beta_{ij1} + \lambda + s_i)z_{ij1} - l_0(1 - z_{ij1}) \le w_j, \qquad \forall i \in V_0, j \in V_\sigma, i \neq j \tag{58}$$

$$e_i \le y_i \le l_i, \qquad \forall i \in V \tag{59}$$

$$0 \le f_j \le f_i - (q_i \sum_{p\in\mathcal{P}_{ij}} x_{ijp}) + Q_e(1 - \sum_{p\in\mathcal{P}_{ij}} x_{ijp}), \qquad \forall i \in V_0, j \in V_\sigma, i \neq j \tag{60}$$

$$0 \le f_0 \le Q_e \tag{61}$$

$$0 \le h_j \le h_i - z_{ij1} + Q_b(1 - z_{ij1}), \qquad \forall i \in V_0, j \in V_\sigma, i \neq j \tag{62}$$

$$0 \le h_0 \le Q_b \tag{63}$$

$$0 \le u_j \le u_i - \gamma_{ijp}u_i - \delta_{ijp}x_{ijp} + (C_e \sum_{\vartheta\in V_0: j\in N} z_{\vartheta j1}) + C_e(1 - x_{ijp}), \ \ \forall (i,j,p)\in\mathcal{P} | i\in V_0, j\in V_\sigma, i\neq j \tag{64}$$

$$\sum_{j\in V_\sigma}\sum_{p\in\mathcal{P}_{ij}} \varphi_{ijp}x_{ijp} \le u_i \le C_e, \qquad \forall i \in N \tag{65}$$

$$u_0 = C_e \tag{66}$$

$$\varphi_{ijp}x_{ijp} \le u_i, \qquad \forall (i,j,p)\in\mathcal{P} \tag{67}$$

$$0 \le v_j \le v_i - \gamma_{ij1}v_i - \delta_{ij1}z_{ij1} + C_b(1 - z_{ij1}), \qquad \forall i \in V_0, j \in V_\sigma, i \neq j \tag{68}$$

$$\sum_{j\in V_\sigma} \varphi_{ij1}z_{ij1} \le v_i \le C_b, \qquad \forall i \in N \tag{69}$$

$$v_0 = C_b \tag{70}$$

$$\varphi_{ij1}z_{ij1} \le v_i, \qquad \forall (i,j,1)\in\mathcal{P} \tag{71}$$

$$x_{ijp} \in \{0,1\}, \qquad \forall (i,j,p)\in\mathcal{P} \tag{72}$$

$$z_{ij1} \in \{0,1\}, \qquad \forall (i,j,1)\in\mathcal{P} \tag{73}$$

$$y_i \ge 0, f_i \ge 0, u_i \ge 0\,, \qquad \forall i \in V \tag{74}$$

$$w_i \ge 0, h_i \ge 0, v_i \ge 0\,, \qquad \forall i \in V\backslash R' \tag{75}$$

The descriptions of the objective functions and constraints (50)-(53), (54)-(56), (57)-(65) and (68)-(69) resemble those given for the original formulation in (1)-(4), (6)-(8), (10)-(18) and (21)-(22), respectively. Constraints (66) and (70) indicate that the ECVs and the BSVs depart the depot at full BCL, respectively. Constraints (67) and (71) respectively ensure that the BCL of an ECV and a BSV at a customer location is larger than the MR-BCL of the path intended to be traversed, respectively. Finally, constraints (72)-(75) define the domains of the decision variables.

Appendix E. Sensitivity of case study results to cost assumptions

The logistics model proposed in this paper relies mainly on the inclusion of BSVs in the service fleet to support the routes of ECVs. Therefore, the main additional cost imposed on the distribution network compared with the baseline scenario model where no BSVs are needed, would pertain to the TCO and operational cost of BSVs, as well as the cost for the inventory of the spare swappable lithium-ion battery packs required. While in the case study we have already adopted a very conservative estimate for an eBSV (i.e.,

40% more expensive than an ECV to purchase and maintain), and despite the fact that the price of lithium-ion battery packs is evidently falling, we have re-optimised scenario III (i.e., coordinated routing of eBSVs and visits to RSs) under 20 different settings of significantly increased cost estimates, and have compared the yielded overall business costs under each of these settings with the cost of the baseline scenario (i.e., Scenario I) in the urban case (i.e., £257.67). The result of these analyses is shown in Figure E.1.

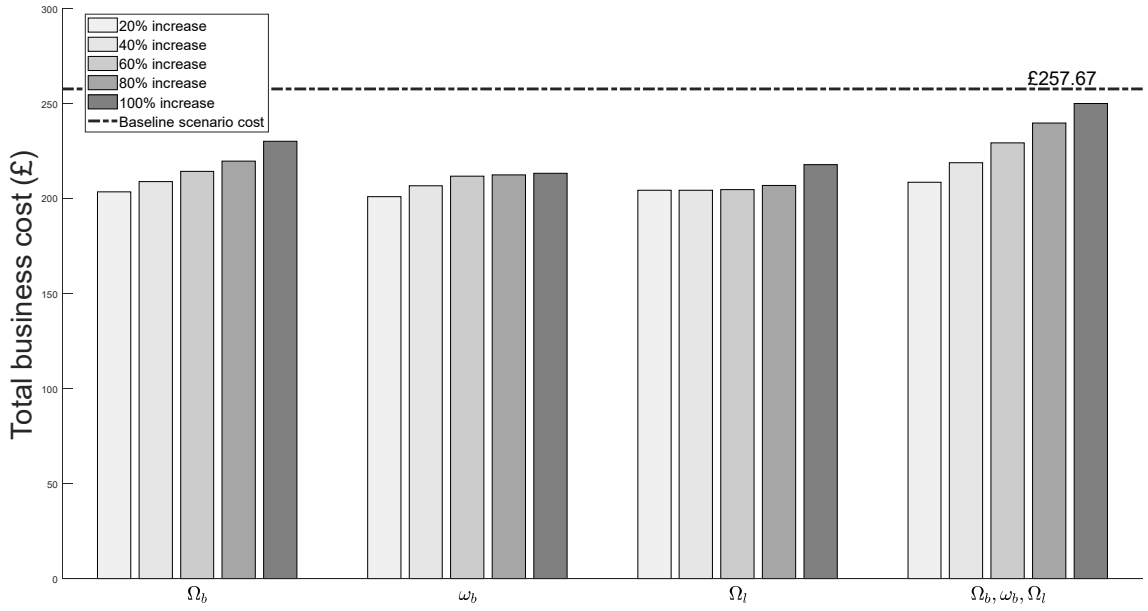

Figure E.1. Sensitivity analysis of BSV and battery pack cost assumptions

As indicated in Figure E.1, the following settings are considered:

- Increasing the current daily cost of an eBSV (Ω_b) in the case study (i.e., £26.91) by 20%, 40%, 60%, 80% and 100%, respectively, while all other cost assumptions remain unchanged.
- Increasing the current operational cost of an eBSV per km (ω_b) in the case study (i.e., £0.15) by 20%, 40%, 60%, 80% and 100%, respectively, while all other cost assumptions remain unchanged.
- Increasing the current daily cost of a lithium-ion battery pack (Ω_l) in the case study (i.e., £3.65) by 20%, 40%, 60%, 80% and 100%, respectively, while all other cost assumptions remain unchanged.
- Increasing simultaneously all the previous cost elements (i.e., Ω_b, ω_b, and Ω_l) by 20%, 40%, 60%, 80% and 100%, while all other cost assumptions remain unchanged.

As it is shown in the figure, even under the extreme case of increasing simultaneously Ω_b, ω_b, and Ω_l by 100%, the total business cost remains below the threshold line set by the baseline scenario.

References

Abdolmaleki, M., Masoud, N., & Yin, Y. (2019). Vehicle-to-vehicle wireless power transfer: Paving the way toward an electrified transportation system. *Transportation Research Part C: Emerging Technologies, 103*, 261-280.

Andelmin, J., & Bartolini, E. (2017). An exact algorithm for the green vehicle routing problem. *Transportation Science, 51(4)*, 1288-1303.

Androutsopoulos, K. N., & Zografos, K. G. (2017). An integrated modelling approach for the bicriterion vehicle routing and scheduling problem with environmental considerations. *Transportation Research Part C: Emerging Technologies, 82*, 180-209.

Bakogiannis, N. (2020). *RETHINKING BATTERY SWAPPING: A view for the future of Automobility*. White Paper retrieved from: https://www.heliev.gr/wp-content/uploads/2020/11/RETHINKING-BATTERY-SWAPPING-A-view-for-the-future-of-Automobility.pdf.

Basso, R., Kulcsár, B., Egardt, B., Lindroth, P., & Sanchez-Diaz, I. (2019). Energy consumption estimation integrated into the Electric Vehicle Routing Problem. *Transportation Research Part D: Transport and Environment 69,* 141-167.

Basso, R., Kulcsár, B., & Sanchez-Diaz, I. (2021). Electric vehicle routing problem with machine learning for energy prediction. *Transportation Research Part B: Methodological, 145*, 24-55.

Bektas, T., & Laporte, G. (2011). The Pollution-Routing Problem. *Transportation Research Part B: Methodological, 45(8)*, 1232-1250.

Bruglieri, M., Pezzella, F., Pisacane, O., & Suraci, S. (2015). A variable neighborhood search branching for the electric vehicle routing problem with time windows. *Electronic Notes in Discrete Mathematics, 47,* 221-228.

Conrad, R. G., & Figliozzi, M. A. (2011, May). The recharging vehicle routing problem. *In Proceedings of the 2011 industrial engineering research conference* (p. 8). IISE Norcross, GA.

Davis, B.A., Figliozzi, M.A., (2013). A methodology to evaluate the competitiveness of electric delivery trucks. *Transportation Research Part E: Logistics and Transportation Review 49*, 8–23.

Desaulniers, G., Errico, F., Irnich, S., & Schneider, M. (2016). Exact Algorithms for Electric Vehicle-Routing Problems with Time Windows. *Operations Research, 64(6)*, 1388-1405.

Drexl, M. (2012). Synchronization in Vehicle Routing-A Survey of VRPs with Multiple Synchronization Constraints. *Transportation Science, 46(3)*, 297-316.

Ehrgott, M. (2005). *Multicriteria optimization* (Second ed.): Springer Science & Business Media.

Erdogan, S., & Miller-Hooks, E. (2012). A Green Vehicle Routing Problem. *Transportation Research Part E: Logistics and Transportation Review, 48(1)*, 100-114.

Felipe, A., Ortuno, M. T., Righini, G., & Tirado, G. (2014). A heuristic approach for the green vehicle routing problem with multiple technologies and partial recharges. *Transportation Research Part E: Logistics and Transportation Review, 71*, 111-128.

Feng, W., & Figliozzi, M. (2013). An economic and technological analysis of the key factors affecting the competitiveness of electric commercial vehicles: A case study from the USA market. *Transportation Research Part C: Emerging Technologies, 26*, 135-145.

Florio, A. M., Absi, N., & Feillet, D. (2020). Routing Electric Vehicles on Congested Street Networks. *Transportation Science*, *Articles in Advance,* 1–19.

Froger, A., Mendoza, J. E., Jabali, O., & Laporte, G. (2019). Improved formulations and algorithmic components for the electric vehicle routing problem with nonlinear charging functions. *Computers & Operations Research, 104*, 256-294.

Garaix, T., Artigues, C., Feillet, D., & Josselin, D. (2010). Vehicle routing problems with alternative paths: An application to on-demand transportation. *European Journal of Operational Research, 204(1)*, 62-75.

Gao, X. J., Zhao, J. L., Shang, W. Z., Wang, T. B., Wang, X. (2 May 2012) A mobile electric vehicle battery swapping van for emergency. CN 201120341622.2,2.

Goeke, D. (2019). Granular tabu search for the pickup and delivery problem with time windows and electric vehicles. *European Journal of Operational Research, 278(3)*, 821-836.

Goeke, D., & Schneider, M. (2015). Routing a mixed fleet of electric and conventional vehicles. *European Journal of Operational Research, 245(1)*, 81-99.

Guo, S., Qian, X., & Liu, J. (2020). Charging-as-a-Service: On-demand battery delivery for light-duty electric vehicles for mobility service. *arXiv preprint arXiv:2011.10665*.

Hiermann, G., Puchinger, J., Ropke, S., & Hartl, R. F. (2016). The Electric Fleet Size and Mix Vehicle Routing Problem with Time Windows and Recharging Stations. *European Journal of Operational Research, 252(3)*, 995-1018.

Hof, J., Schneider, M., & Goeke, D. (2017). Solving the battery swap station location-routing problem with capacitated electric vehicles using an AVNS algorithm for vehicle-routing problems with intermediate stops. *Transportation Research Part B: Methodological, 97*, 102-112.

Hung, Y. C., Lok, H. P., & Michailidis, G. (2021). Optimal routing for electric vehicle charging systems with stochastic demand: A heavy traffic approximation approach. *European Journal of Operational Research, 73*.

ITF (2018), *Towards Road Freight Decarbonisation: Trends, Measures and Policies*, OECD/ITF, Retrieved from: https://www.itf-oecd.org/sites/default/files/docs/towards-road-freight-decarbonisation_0.pdf.

Jie, W., Yang, J., Zhang, M., & Huang, Y. (2019). The two-echelon capacitated electric vehicle routing problem with battery swapping stations: Formulation and efficient methodology. *European Journal of Operational Research, 272(3)*, 879-904.

Keskin, M., & Çatay, B. (2016). Partial recharge strategies for the electric vehicle routing problem with time windows. *Transportation Research Part C: Emerging Technologies, 65*, 111-127.

Keskin, M., Çatay, B., & Laporte, G. (2021). A simulation-based heuristic for the electric vehicle routing problem with time windows and stochastic waiting times at recharging stations. *Computers & Operations Research, 125*, 105060.

Keskin, M., Laporte, G., & Çatay, B. (2019). Electric vehicle routing problem with time-dependent waiting times at recharging stations. *Computers & Operations Research, 107*, 77-94.

Koç, Ç., & Karaoglan, I. (2016). The green vehicle routing problem: A heuristic based exact solution approach. *Applied Soft Computing, 39*, 154-164.

Kosmanos, D., Maglaras, L. A., Mavrovouniotis, M., Moschoyiannis, S., Argyriou, A., Maglaras, A., & Janicke, H. (2018). Route optimization of electric vehicles based on dynamic wireless charging. *IEEE Access, 6*, 42551-42565.

Kucukoglu, I., Dewil, R., & Cattrysse, D. (2021). The electric vehicle routing problem and its variations: A literature review. *Computers & Industrial Engineering, 107650*.

Kullman, N., Goodson, J., Mendoza, J.E., (2018). *Dynamic electric vehicle routing with mid-route recharging and uncertain availability*. ODYSSEUS 2018 - Seventh International Workshop on Freight Transportation and Logistics. Cagliari, Italy.

Lee, D.Y., Thomas, V.M., Brown, M.A., 2013. Electric urban delivery trucks: Energy use, greenhouse gas emissions, and cost-effectiveness. *Environmental science & technology, 47(14),* 8022–8030.

Lin, B., Ghaddar, B., & Nathwani, J. (2021). Electric vehicle routing with charging/discharging under time-variant electricity prices. *Transportation Research Part C: Emerging Technologies, 130*, 103285.

Lu, G. J., & Zhou, Y. P. (16 October 2013). *A electric vehicle with bottom lateral linkage battery swapping and its battery swapping devices*. CN 201310164242.X.

Martins, E. Q. V. (1984). On a Multicriteria Shortest-Path Problem. *European Journal of Operational Research, 16(2)*, 236-245.

Montoya, A., Gueret, C., Mendoza, J. E., & Villegas, J. G. (2017). The electric vehicle routing problem with nonlinear charging function. *Transportation Research Part B: Methodological, 103,* 87-110.

Pelletier, S., Jabali, O., & Laporte, G. (2019). The electric vehicle routing problem with energy consumption uncertainty. *Transportation Research Part B: Methodological, 126*, 225-255.

Raeesi, R., & O'Sullivan, M. J. (2014). Eco-logistics: environmental and economic implications of alternative fuel vehicle routing problem. *International Journal of Business Performance and Supply Chain Modelling, 6(3-4)*, 276-297.

Raeesi, R., & Zografos, K. G. (2020). The electric vehicle routing problem with synchronised mobile battery swapping. *Transportation Research Part B: Methodological, 140,* 101-129.

Raeesi, R., & Zografos, K. G. (2019). The multi-objective Steiner pollution-routing problem on congested urban road networks. *Transportation Research Part B: Methodological, 122,* 457-485.

Salimifard, K., & Raeesi, R. (2014). A green routing problem: optimising CO_2 emissions and costs from a bi-fuel vehicle fleet. *International Journal of Advanced Operations Management, 6(1)*, 27-57.

Sanguesa, J. A., Torres-Sanz, V., Garrido, P., Martinez, F. J., & Marquez-Barja, J. M. (2021). A Review on Electric Vehicles: Technologies and Challenges. *Smart Cities, 4(1)*, 372-404.

Schiffer, M., Stütz, S., & Walther, G. (2017). *Are ECVs Breaking Even? - Competitiveness of Electric Commercial Vehicles in Retail Logistics*. Technical Report G-2017-47. RWTH Aachen University. Aachen. retrieved from: https://publications.rwth-aachen.de/record/691766.

Schiffer, M., & Walther, G. (2017). The electric location routing problem with time windows and partial recharging. *European Journal of Operational Research, 260(3)*, 995-1013.

Schneider, M., Stenger, A., & Goeke, D. (2014). The Electric Vehicle-Routing Problem with Time Windows and Recharging Stations. *Transportation Science, 48(4)*, 500-520.

Shao, S. J., Guo, S. Y., Qiu, X. S. (2017). A mobile battery swapping service for electric vehicles based on a battery swapping van. *Energies 10 (10)*, 1667.

Solomon, M. M. (1987). Algorithms for the vehicle routing and scheduling problems with time window constraints. *Operations research, 35(2)*, 254-265.

Sweda, T. M., Dolinskaya, I. S., & Klabjan, D. (2017). Adaptive routing and recharging policies for electric vehicles. *Transportation Science, 51(4)*, 1326-1348.

Yang, J., & Sun, H. (2015). Battery swap station location-routing problem with capacitated electric vehicles. *Computers & Operations Research, 55*, 217-232.

Worley, O., Klabjan, D., & Sweda, T. M. (2012). *Simultaneous vehicle routing and charging station siting for commercial electric vehicles.* In 2012 IEEE International Electric Vehicle Conference (pp. 1-3), Greenville, NC.

Xiao, Y., Zhang, Y., Kaku, I., Kang, R., & Pan, X. (2021). Electric vehicle routing problem: A systematic review and a new comprehensive model with nonlinear energy recharging and consumption. *Renewable and Sustainable Energy Reviews, 151*, 111567.

Zhang, X., Cao, Y., Peng, L., Li, J., Ahmad, N., & Yu, S. (2020). Mobile charging as a service: A reservation-based approach. IEEE *Transactions on Automation Science and Engineering, 17(4)*, 1976-1988.

Zündorf, T., 2014. *Electric vehicle routing with realistic recharging models*. Karlsruhe Institute of Technology, Karlsruhe, Germany. Master's thesis.